

Review

# Electrochemical Approaches for the Recovery of Metals from Electronic Waste: A Critical Review

Varun Rai <sup>1</sup>, Daobin Liu <sup>1</sup>, Dong Xia <sup>1</sup>, Yamuna Jayaraman <sup>1</sup> and Jean-Christophe P. Gabriel <sup>1,2,\*</sup>

<sup>1</sup> SCARCE Laboratory, Energy Research Institute @ NTU (ERI@N), Nanyang Technological University, Singapore 637459, Singapore; varun.raiantu.edu.sg (V.R.); daobin.liuantu.edu.sg (D.L.); xiadong@ntu.edu.sg (D.X.); yamuna.jayaraman@ntu.edu.sg (Y.J.)

<sup>2</sup> LICSEN, NIMBE, CNRS, CEA, Université Paris-Saclay, 91191 Gif-sur-Yvette, France

\* Correspondence: jean-christophe.gabriel@cea.fr

**Abstract:** Electronic waste (e-waste) management and recycling are gaining significant attention due to the presence of precious, critical, or strategic metals combined with the associated environmental burden of recovering metals from natural mines. Metal recovery from e-waste is being prioritized in metallurgical extraction owing to the fast depletion of natural mineral ores and the limited geographical availability of critical and/or strategic metals. Following collection, sorting, and physical pre-treatment of e-waste, electrochemical processes-based metal recovery involves leaching metals in an ionic form in a suitable electrolyte. Electrochemical metal recovery from e-waste uses much less solvent (minimal reagent) and shows convenient and precise control, reduced energy consumption, and low environmental impact. This critical review article covers recent progress in such electrochemical metal recovery from e-waste, emphasizing the comparative significance of electrochemical methods over other methods in the context of an industrial perspective.

**Keywords:** e-waste; recycling; leaching; metal recovery; electrodeposition; electrowinning; supercritical fluids



**Citation:** Rai, V.; Liu, D.; Xia, D.; Jayaraman, Y.; Gabriel, J.-C.P. Electrochemical Approaches for the Recovery of Metals from Electronic Waste: A Critical Review. *Recycling* **2021**, *6*, 53. <https://doi.org/10.3390/recycling6030053>

Academic Editor: Ana Paula Paiva

Received: 7 July 2021

Accepted: 3 August 2021

Published: 9 August 2021

**Publisher's Note:** MDPI stays neutral with regard to jurisdictional claims in published maps and institutional affiliations.



**Copyright:** © 2021 by the authors. Licensee MDPI, Basel, Switzerland. This article is an open access article distributed under the terms and conditions of the Creative Commons Attribution (CC BY) license (<https://creativecommons.org/licenses/by/4.0/>).

## 1. Introduction

E-waste is very heterogeneous in nature, consisting of various systems containing diverse categories of metal, plastics, and ceramics, which are therefore considered potential secondary resources. PCBs are valuable sub-systems of e-waste, which often contain more than sixty different chemical elements [1]. E-waste management and recycling are critical to environmental sustainability and reducing carbon emissions. According to the Global-E-waste-Monitor 2020 report by the United Nations University (UNU) and the United Nations Institute for Training and Research (UNITAR) and the International Solid Waste Association (ISWA), 53.6 million metric tonnes (Mt) of e-waste were generated globally in 2019, up 9.2 Mt from the previous five years, and only 17.4% of e-waste was formally collected and recycled [2]. At the Plenipotentiary Conference 2018, the highest policy-making body of the International Telecommunication Union (ITU), there was a proposal to bring the global e-waste recycling target up to 30% by 2023. Therefore, the recycling of e-waste is gaining prominence in order to reduce the increasing load on the environment and landfill sites. Recycling e-waste not only involves the recovery of metals but also involves the other ingredients. It is equally important to note that a single recycling strategy cannot be applied to all e-waste all over the world. However, to increase the widespread feasibility of recycling of e-waste, processes should focus on the minimal release of toxic and hazardous substances along with adhering to an economically viable operational cost.

Leachate solutions from the acid digestion of e-waste contain multiple metal ions that vary highly from one lot to the other, which poses great challenges in the selective recovery of metals in pure forms. Electrochemical processes (electrodeposition/electrowinning) involve selective metal recovery with reduced solvent and energy consumption from the

leachate solution of e-waste [3–7]. Both electrowinning and electrorefining are the primary methods for metal purification (e.g., Cu, Zn, Co, Au, and so forth), from an aqueous solution containing a high metal ion concentration, at the industrial scale. In addition, the electrochemical method reduces the use of environmental pollution reagents [8]. Electrodeposition uses the selective reduction potential of each metal ion, where constant potential is applied to electrode surfaces immersed in leachate (electrolyte) solution, in order to reduce metal ions. Moreover, conducting electrodeposition in an aqueous electrolyte solution at a large scale is always preferred due to inexpensive water solvent and the smaller environmental and fire hazards compared to an organic solvent-based electrolyte solution. Despite the advantages of electrodeposition in aqueous solvent, the low breakdown voltage ( $E_{\text{breakdown}} = 1.23 \text{ V, H}_2\text{O}$ ) of water limits its usage, in terms of width of the accessible potential window. Therefore, non-aqueous solvents (e.g., dimethyl sulfoxide, dimethylformamide, propylene carbonate) and ionic liquids, and their higher breakdown voltage, are employed in selective metal electrodeposition.

Regarding metal recovery, prior to any electrochemical processes, it is very important to ensure that the metals considered are in a soluble ionic form [9]. A metal leaching processes step is required, which depends on the particle size of the grinded waste as well as on the lixiviant nature, concentration, treatment time, temperature, pH, solid–liquid ratio, agitation, and redox potential. These have been reviewed elsewhere [10–12].

To add to the complexity of e-waste recycling, it should be noted that there is a lack of standard processes for the measurement of e-waste's metal content. This leads to great variations from one study to the other but can lead to some metal being totally overlooked in some reports (such as refractory metals—Ta, Nb, Mo, W, or Re), as they are not dissolved or are only a little dissolved during the leaching steps. However, some efforts are on-going to resolve this issue [13].

Efficient electrochemical recovery of pure metals from e-waste leachate highly depends on the quality and uniformity of metal ions (e.g., single metal ions) in the leachate. The presence of multiple metal ions in the leachate is however inevitable due to the very nature of e-waste, which incorporates wide range of metals that have fairly diverse properties. Therefore, to improve the quality and purity of metal electrodeposition from e-waste, leachates with multiple metal ions are chemically processed to obtain leachate with single metal ions. To that end, metal ions are selectively transferred and preconcentrated from the leachate into aqueous, non-aqueous, or ionic liquid systems to conduct electrodeposition in the respective latter medium. Metal recovery through the electrodeposition of metals in ionic liquids (ILs) from e-waste is employed to achieve high selectivity and low operating temperature conditions [14]. Electrochemical metal recovery using ionic liquid involves transferring the metallic ions from the leachate into ionic liquid systems for electrolysis.

Overall, electrochemical approaches in metal recovery have several advantages such as uniformity in metal deposition, high purity, automation, easy control, cost effectiveness, and relatively fast processing time. Electrodeposition can be applied over non-uniform complex electrode surfaces. However, the electrodeposition of metals suffers from the following limitations: (i) adsorption of non-electroactive particles on the electrode; (ii) problems associated with over-potential measurements; (iii) current density variability throughout the electrode surface due to surface roughness at the macro-, meso-, and microscales; and (iv) nucleation rates distribution between growth steps. Alloy formation and impurity trapping during metal electrodeposition in leachate solution are also inevitable. Therefore, suitable pH adjustments and further chemical treatments are applied to widen potential reduction gaps among various metal ions to enable the deposition of the only targetted metal from leachate. Moreover, when the electrodeposited metal thickness remains thin (not exceeding  $1 \mu\text{m}$ ), problems associated with over-potential and current distribution are minimal. However, thicker and maximum electrodeposited metals are desired in the metal recovery processes for industrial applications and for the compensation of economic recovery costs. Thus, thicker metal dispositions have the problems of non-uniformity and the inclusion of non-electroactive molecules as impurities, e.g., hydrogen inclusion into the deposits [15,16]. It is important to know that the

electrochemical process as the potential of improving the quality of recovered metals by reducing impurities, which adds significant value to the recovered materials. Calculating the cost and energy consumption of metal recovery using electrochemical processes and comparing them to other methods requires information about the cost of the chemicals involved (including their disposal/recycling), human capital, as well as the time and quality of therecovered material, which can vary a lot from one place or metal to another. However, the minimum viable smelting operation in pyrometallurgy requires an annual throughput of 30 kt/year, and the capital investment is around USD 15 million, while the electrochemical recovery processes involves 20 kt/year with the capital investment around USD 6.8 million [17–19]. Furthermore, by considering the quality of the recovered metal, the electrochemical process known as electrowinning leads to copper deposits of up to 99.99% purity in contrast to the precipitation process and pyro metallurgical smelting, which only results in the 85–90% and 50–75% purity ranges, respectively [20].

Electrochemical approaches based on metal recovery from e-waste have also some other limitations that are associated with the very nature of e-waste recycling processes. The recovery of a smaller concentration of target metal in leachates and the use of hazardous and corrosive lixivants (e.g.,  $\text{CN}^-$  for gold recovery) are very serious concerns for the industry as well as for the environment. Hence, the effective sorting and pre-treatment of e-waste are very critical to overcome downstream processing challenges and costs. Figure 1 shows an overview of the metal recovery processes and pre-treatment steps for e-waste using pyrometallurgy, hydrometallurgy, and bio-hydrometallurgy. The electrochemical process follows the leaching step of hydrometallurgy. The metal recovery strategy for e-waste by electrodeposition depends on the types of metal, their combinations, the hydrometallurgical extraction process, and the lixivants used. However, by employing the simultaneous electro-oxidation of metal from e-waste in the anodic half-cell and electrochemical reduction of dissolved target metal ions in cathodic half-cell, electro-oxidative leaching and metal deposition are able to be conducted simultaneously. In the next section, the nature and proportion of metals in e-waste (e.g., printed circuit boards) that can be recovered through electrochemical approaches, as well as the associated processes' limitations are critically reviewed from both an academic and industrial outlook.

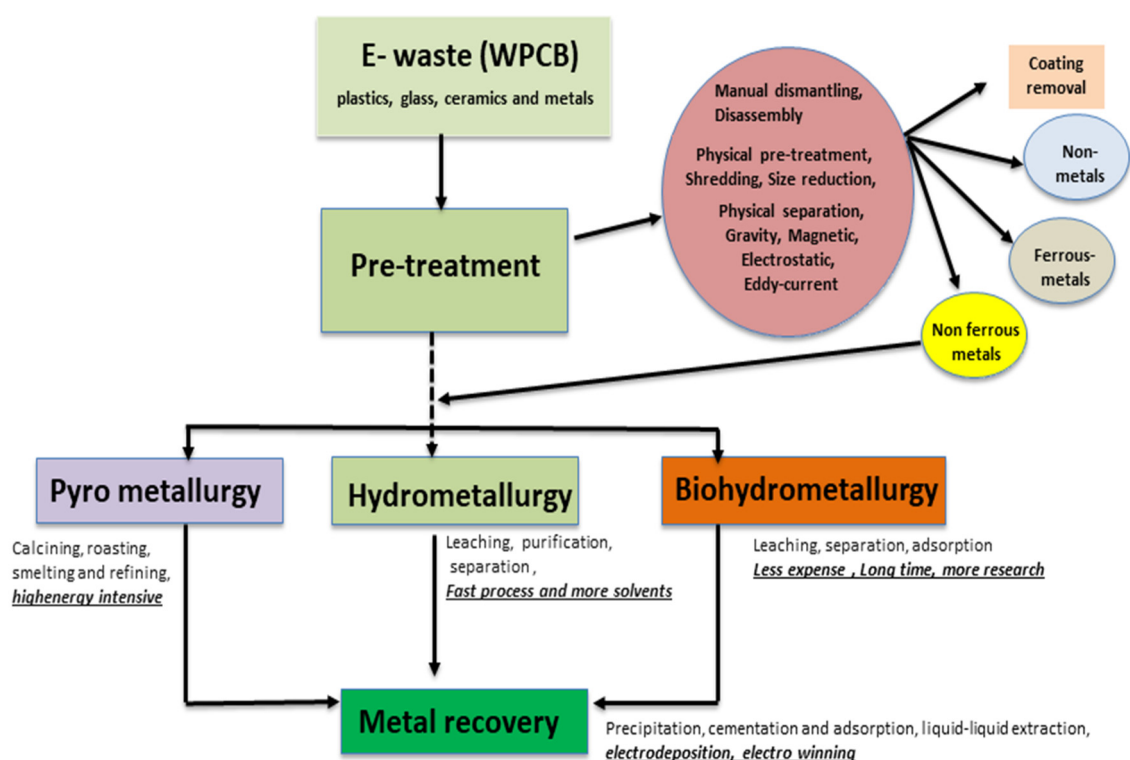


Figure 1. Scheme of metal recovery from e-waste (printed circuit boards) [9].

## 2. Metals in E-Waste That Can Be Recovered Electrochemically

Metals in e-waste can be categorized into three major categories: base metals, precious metals, and rare earth elements (REEs). Base metals constitute a large fraction ~30 wt% e.g., Fe, Cu, Al, Ni in e-waste. Precious metals constitute around 0.1–1 wt%, e.g., Au, Ag, Pd, and Ir, and rare earth elements, e.g., La, Dy, Nd, Pr, Gd, Sc, and Y, are present even in smaller wt% fraction [10,21–24]. Apart from the above categories, metals are also classified as critical or non-critical, considering potential threat in their supply and procurement for essential high-tech product development. Although the classification is country dependant, typical critical metals include In, Co, Ga, W, Ta, and most rare earth elements [9]. Toxic metals such as arsenic, mercury, antimony, cadmium, or lead are also found in ewastes, sometimes even in large amounts (solder), which creates complexity in e-waste treatment, disposal, recovery, and recycling. Major devices found in e-waste are computers, laptops, mobile phones, flat screens, batteries, lighting LEDs, LCDs, fluorescence lamps, cathode ray tubes, PCBs, etc.

Metals present (%wt average) in e-waste (PCB) as reported in literature [25] and their appropriate medium for electrochemical recovery are reported in Table 1. Aqueous and non-aqueous media are the common electrolytic media used in electrodeposition techniques for metal recovery. The aqueous medium's higher ionic mobility and conductivity make it ideal for depositing metals such as Au, Ag, Fe, Cu, Ni, Co, Zn, W, and Cr [26]. However, it does not deposit metals such as Al, which has a greater negative redox potential of  $-1.67$  V and is also water sensitive, which may quickly lead to the building of a passivation oxidation layer on its surface, slowing or even stopping its electrodeposition in aqueous solutions [27]. Ionic liquids have emerged as promising solvents for addressing this issue [28]. Hence, metals such as In, Ga, Ta, Pd, Ir, Gd, La, and Pr have previously been electrodeposited in ionic liquid media [29]. Na and Ca metals are even more difficult to recover electrochemically, requiring the use of molten salt media for their recovery.

Table 2 shows some metals of particular interest present in various components of e-waste [10,30]. It is indeed very important to know the composition of e-waste before employing any given recycling and metal recovery strategy. Hence, metal profiling is a prerequisite for a proper cost analysis of metal recovery and e-waste recycling. E-waste are therefore categorized and separated according to their content and value based on metallic composition. Generally, more focus is given by the industry to the recovery of gold, silver, and copper due to their abundance in e-waste and their established recovery processes. Indeed, the recovery of rare earth elements remains challenging due to their lower amounts and associated recovery/separation costs. To make it economically viable, there is yet a need for new technologically and economically efficient processes steps to preconcentrate rare earth elements during the physical and mechanical pre-treatment of e-wastes.

**Table 1.** Metals present (% average) in e-waste PCB reported in literature. Ionic liquid full names and abbreviations are as such: n-butyl-n-methylpyrrolidinium bis(trifluoromethylsulfonyl)imide (BMP TFSA), 1-Ethyl-3-methylimidazolium bis(trifluoromethylsulfonyl)imide (EMIM TFSA), 1-Ethyl-3-methylimidazolium chloride (EMIm Cl), 1-Ethyl-3-methylimidazolium—tetrafluoroborate (EMIM Cl-Bf4), 1-Butyl-3-methylimidazolium tetrafluoroborate (BMIM Bf4).

Metal Content <i>w/w</i>	[31]	[32]	[33]	[34]	[35]	[36]	[37]	[38]	[39]	[40]	[41]	[42]	[43]	[25]	Aver.	Stand. Dev.	Medium	Electrolyte
Cu (%)	19	20	22	12.5	26.8	15.6	19.6	28.7	27.6	14.6	12.5	19.19	28	14.2	20.0	5.8	Aqueous	CuSO <sub>4</sub> , potash alum and H <sub>2</sub> SO <sub>4</sub> [44]
Al (%)	4.1	2	–	2.04	4.7	–	2.8	1.7	–	–	2.3	7.06	2.6	–	3.2	1.7	Ionic liquid	AlCl <sub>3</sub> and EMIm Cl [45]
Pb (%)	1.9	2	1.5	2.7	–	1.35	3.9	1.3	–	2.9	2.4	1.01	–	2.5	2.1	0.8	–	–
Zn (%)	0.8	1	–	0.08	1.5	0.16	2.1	–	2.7	–	–	0.73	–	0.18	1.0	0.9	Aqueous	ZnCl <sub>2</sub> and sulphuric acid [44]
Ni (%)	0.8	2	0.3	0.7	0.47	0.28	0.38	–	0.3	1.6	0.39	5.35	0.26	0.41	1.0	1.4	Aqueous	NiSO <sub>4</sub> , NiCl <sub>2</sub> and boric acid [46]
Fe (%)	3.6	8	3.6	0.6	5.3	1.4	11.4	0.6	2.9	4.7	3.2	3.56	0.08	3.08	3.7	3.0	Aqueous	FeCl <sub>3</sub> and HCl [47]
Sn (%)	1.1	4	2.6	4	1	3.2	3.6	3.8	–	5.6	1.4	2.03	–	4.79	3.1	1.4	Aqueous	SnCl <sub>2</sub> (NH <sub>4</sub> ) <sub>3</sub> -citrate [48]
Sb (%)	–	–	–	–	0.06	–	–	–	–	–	–	–	–	0.05	0.05	0.007	–	–
Cr (%)	–	–	–	–	–	–	0.005	–	–	0.35	–	–	–	–	0.18	0.2	Aqueous	CrO <sub>3</sub> and H <sub>2</sub> SO <sub>4</sub> [49]
Na (%)	–	–	–	–	–	–	–	–	–	–	–	–	–	0.48	0.48	N/A	–	–
Ca (%)	–	–	–	–	–	–	1.13	–	1.4	–	–	–	–	1.69	1.4	0.2	–	–
Ag (ppm)	5210	2000	–	300	3300	1240	500	79	–	450	–	100	135	317	1239.2	1654.0	Aqueous	Ag salts and KCN [50]
Au (ppm)	1120	1000	350	–	80	420	300	68	–	205	–	70	29	142	344	376.9	Ionic liquid	K [Au (CN) <sub>2</sub> ] and EMIM TFSA [51]
Pt (ppm)	–	–	–	–	–	–	–	0	–	–	–	–	–	–	0	N/A	Ionic liquid	H <sub>2</sub> PtCl <sub>6</sub> and BMIM BF <sub>4</sub> [52]
Cd (ppm)	–	–	–	–	–	–	–	–	–	–	–	–	–	1183	1183	N/A	–	–
K (ppm)	–	–	–	–	–	–	–	–	–	–	–	–	–	180	180	N/A	–	–
In (ppm)	–	–	–	–	–	–	500	–	–	–	–	–	–	–	500	N/A	–	–
Mn (ppm)	–	–	–	–	–	–	9700	–	4000	–	–	–	–	81	4593.6	4836.9	–	–
Se (ppm)	–	–	–	–	–	–	–	–	–	–	–	–	–	21	21	N/A	–	–
As (ppm)	–	–	–	–	–	–	–	–	–	–	–	–	–	11	11	N/A	–	–
Mg (ppm)	–	–	–	500	–	–	1000	–	–	–	–	–	–	–	750	353.5	–	–
Pd (ppm)	–	50	–	–	–	–	–	33	–	220	–	–	–	–	101	103.4	Ionic liquid	PdCl <sub>2</sub> , AgCl and EMIM Cl-BF <sub>4</sub> [53]
Co (ppm)	–	–	–	–	–	–	300	–	–	–	–	400	–	–	350	70.7	–	–
Ti (ppm)	–	–	–	–	–	–	–	–	–	–	–	400	–	–	400	N/A	Ionic liquid	TiCl <sub>4</sub> and BMIM TFSA [54]
Total metals (%)	31.9	39.3	30.1	22.6	40.2	22.2	46.5	36.1	35.3	30.1	22.5	39.1	31.1	27.6	32.4	7.3	–	–

**Table 2.** Rare earth metals and other critical metals present in various components of e-waste.

Components of E-Waste	Rare Earth Metals/Critical Metals	Amount (~ppm)
LEDs, CRT/fluorescence lamps, batteries	La	91
CRT/fluorescence lamps, batteries	Ce	72
Electric gas lamp	Th	6
Speakers/magnets, batteries/fluorescence lamps	Pr	
Speakers/magnets	Gd	
Speakers/magnets/batteries	Nd	–
Speakers/magnets/capacitors	Dy	–
CRT/fluorescence lamps	Eu	
LEDs, CRT/fluorescence lamps	Tb	10
CRT/fluorescence lamps	Y	10
Discharge lamps	Sc	55
LEDs	Ga	35
PCBs/capacitors and some high-power resistors	Ta	–

### 3. Electrodeposition: Principle and Mechanism

In this section, we briefly cover the principal mechanism and underlying Equations (1) and (2) for electrodeposition, which are very important in the next section discussing electrochemical approaches for metal recovery. The electrodeposition process is conventionally conducted in a three-electrodes electrochemical cell set up comprising of a reference, a working, and a counter electrode. The working electrode can act as the cathode, and the counter electrode works as the anode. In electrodeposition, metal ions ( $M^{n+}$ ), dissolved in a liquid phase (aqueous, organics, or molten salts), are reduced to form a metal electrodeposit, also called a cathodic deposit ( $M^0$ ), at the cathode by applying an external electrical potential [55] (Equation (1)).



This reversible electrochemical reduction–deposition is governed by its equilibrium potential ( $E^{eq}$ ), which depends on the chemical activities of the metal ions ( $a_{M^{n+}}$ ) and the deposited metallic atoms ( $a_M$ ) and follows the Nernst equation (Equation (2)):

$$E^{eq} = E^0 + \frac{RT}{nF} \ln \frac{a(Mn^{+})_{ox}}{a(M)_{red}} \quad (2)$$

where  $R$  is the ideal gas constant ( $R = 8.314 \text{ J K}^{-1} \text{ mol}$ ),  $T$  is the temperature in Kelvin,  $F$  is the Faraday constant ( $F = 96,485.339 \text{ C mol}^{-1}$ ), and  $E^0$  is the normal electrode potential measured as the individual electrode potential of the reversible electrode in standard conditions (concentration of 1 M or 1 bar pressure for gases, temperature of 298 K) [56,57]. Figure 2 shows a schematic representation of the electrodeposition process (A) and its detailed mechanism (B). As shown in Figure 2B, the electrodeposition process for recovering valuable metals consists of four intermediate stages: (i) the potential induced metal ion transport from the electrolyte to the cathode; (ii) the stripping of the ion hydration layer at the cathode–solution interface; (iii) the metal atom clustering by the electron transfer from the cathode to the adsorbed metal ions; and (iv) the growth of metal clusters and transformation into the bulk aggregations [16,58].

The electrodeposition of metals primarily depends on electrical potential and electron current distribution at the electrode, as uniform current distribution leads to homogeneous metal deposition of uniform thickness. The current distribution at the electrode relies on the metal ion transport property toward the electrode, the polarization at the electrode, the geometry of the electrochemical cell, the position and shape of electrodes in the cell, the properties of the electrolyte, and the electrolyte/electrode interface. Figure 3

shows the effect of different current distributions (primary, secondary, and tertiary) on the electrodeposit thickness over the electrode surface. The current distribution over the electrode affects the thickness distribution of the electrodeposited metals that subsequently controls the local current density on the electrode's surface. The current and resistance of the electrolyte from anode to cathode determines the primary current distribution. The secondary current distribution is controlled by the resistance of the electrolyte path and the reaction overpotential. The tertiary current distribution depends on the movement of ions between the cathode and the solution through the diffusion layer. Thus, these three current distributions play critical roles at different extents in the overall cathodic electrodeposition process.

Overpotential (OPD) and underpotential (UPD) deposition refer to electrodeposition at different potentials than the equilibrium (Nernst) potential for the reduction of the target metal ions [59]. Overpotential is the potential difference (voltage) between thermodynamically determined reduction potential and the potential at which the redox event is experimentally observed. It arises due to a concentration gradient of the reactants, or the products, in the bulk electrolyte and at the electrode surface, which is usually due to a slow mass transport while the cell reaction proceeds. UPD occurs at a less negative potential compared to the equilibrium potential for the reduction of the metal. In this case, a metal is deposited onto another metal substrate more easily than it can be deposited onto itself. UPD arises when the electrodeposited metal has a stronger interaction with the electrode's metal surface than with itself.

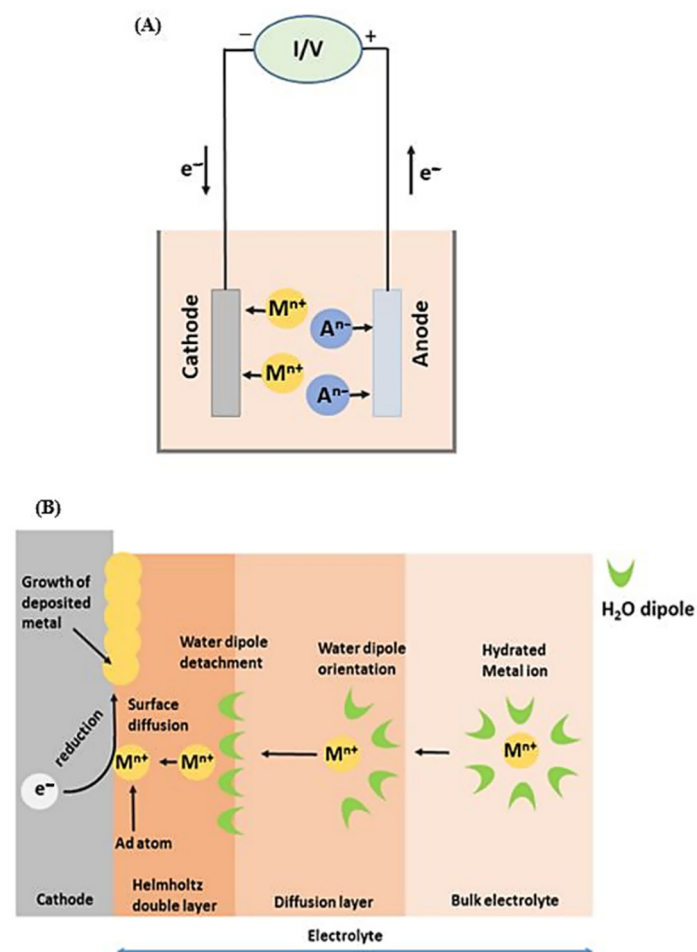
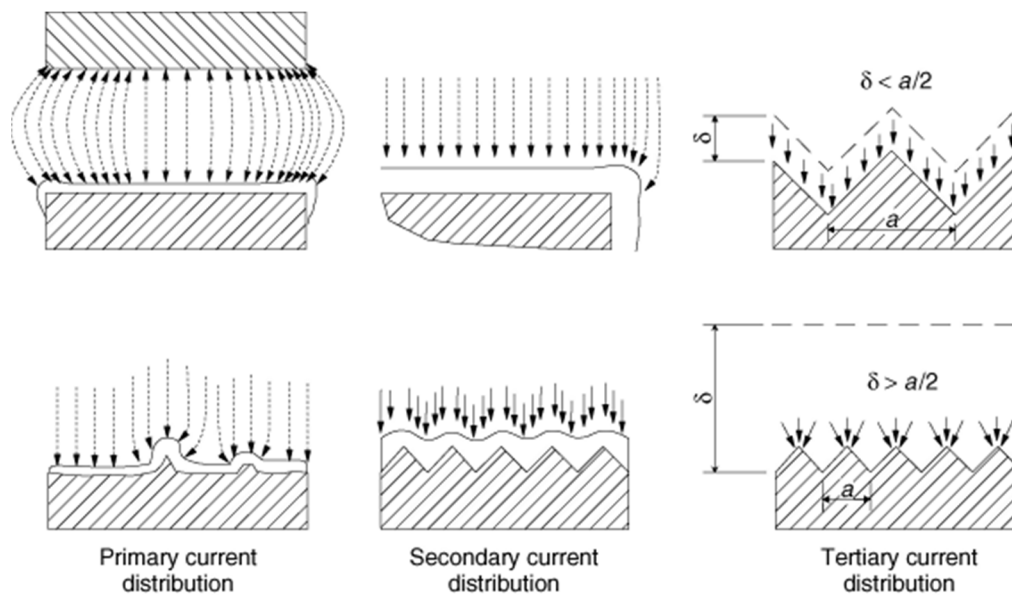


Figure 2. Schematic representation of electrodeposition process (A) and mechanism details (B).



**Figure 3.** The effect of different current distributions (primary, secondary, and tertiary) on the electrodeposit thickness over the electrode surface. Reproduced with permission [16]. Copyright 2007, Wiley.

#### 4. The Various Approaches for Electrochemical Recovery of Metals

##### 4.1. Potential Controlled and Current Controlled Electrodeposition

Potential controlled electrodeposition, known as the potentiostatic process, applies a constant voltage in which the current density may change as a function of time. It is widely used for fundamental research since the potential is the driving force that can determine which electrochemical reaction occurs, hence enabling highly selective metal recovery. By contrast, current controlled electrodeposition, known as the galvanostatic process, imposes a constant current and therefore a constant electrochemical reaction rate, regardless of the reactions that occur [60]. The co-deposition of different metal species could simultaneously occur under the constant current density in complex systems, such as in e-waste leaching solutions. To avoid such co-deposition, one must be careful to have a sufficient excess of metal ions to be deposited near the cathode compared to the current density employed. Current controlled electrodeposition is mostly used for electrocrystallization to obtain large crystals [60] as well as in electrodeposition at the industrial scale because of its easy-to-control energy consumption [61]. Thus, we can conclude that the potential controlled electrodeposition is an important approach in the recovery of high purity metals from the complex leaching solution. For example, the precious metal Pd could be selectively recovered from waste multilayer ceramic capacitors (MLCCs) using the potential controlled electrodeposition method [62]. The reduction potentials of all of the leached-out metals were widely different in the  $\text{HNO}_3$  leaching solution, with  $\text{Cu}^{2+}$ ,  $\text{Pd}^{2+}$  and  $\text{Pb}^{2+}$  being prominent. The authors studied the electrodeposition behaviour of Pd at a titanium electrode and investigated the effect of agitation speeds by calculating the thickness of the diffusion region. Figure 4 shows the linear sweep voltammogram (LSV) curves of the simulated solution with respect to  $\text{HNO}_3$ ,  $\text{Pd}^{2+}$ , and  $\text{Cu}^{2+}$  in  $\text{HNO}_3$ , which confirms the reduction of  $\text{Pd}^{2+}$  into metallic Pd at  $-0.13$  V. Overall, high-purity Pd metal (>99%) was obtained with a recovery rate of 99.02% under optimal conditions (applied potential of 0.25 V, agitation speed of 240 rpm, and 0.5 M  $\text{HNO}_3$ ).

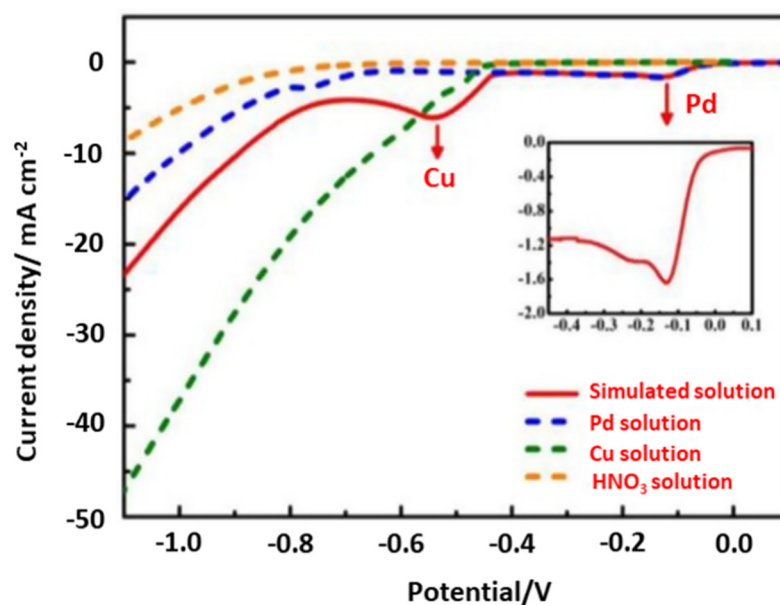


**Figure 4.** The linear sweep voltammogram (LSV) curves of the simulated solution, a  $\text{Pd}^{2+}$  solution,  $\text{Cu}^{2+}$  solution, and  $\text{HNO}_3$ . Reproduced with permission [62]. Copyright 2020, Elsevier.

Selective recovery of metals (e.g., Cu) could only be achieved by current controlled electrodeposition for specific leaching systems. In such cases, and using constant direct current (DC), the recovery efficiency of Cu from e-waste could reach as high as 95% with a Cu purity higher than 99%, in an ammonia-based electrolyte [63,64]. This is mainly due to the selective extraction of Cu by ammonium ions during the initial leaching process. Similarly, the current controlled electrodeposition method was used to selectively reduce  $\text{Fe}^{2+}$  in the leachate derived from an aqueous solution containing a mixture of  $\text{Fe}^{2+}$  and  $\text{Nd}^{3+}$ , obtained from the leaching of wasted permanent magnets (Nd-Fe-B) [65]. The reduction potential of  $\text{Fe}^{2+}$  was selectively adjusted by changing the pH of the medium through the addition of ammonium sulfate ( $(\text{NH}_4)_2\text{SO}_4$ ) and sodium citrate ( $\text{Na}_3\text{Cit}$ ). The resulting solution was therefore enriched in a  $\text{Nd}^{3+}$ , depleted in  $\text{Fe}^{2+}$ , and was further treated with a  $\text{Na}_2\text{SO}_4$  solution to precipitate  $(\text{NdNa})(\text{SO}_4)_2$ .

Generally, the efficiency of electrodeposition can be evaluated from the aspects of current density, current efficiency (the proportion of current used for metal deposition), and the speed of mass transfer [66]. The operating parameters in the process, such as the initial concentration of metal salts, the composition of electrolytes, the voltage, the flow rate, the pH, and the temperature all significantly affect the efficiency of electrodeposition [67]. Among these parameters, the voltage plays a critical role in the recovery of valuable metals from the solution due to its correlation with the current density. Hence, by employing the Taguchi method, Peng et al. (2014) demonstrated that the voltage is the most influential parameter and that it more highly affects the recovery efficiency of nickel when compared to pH or the initial concentration of nickel salts. This is shown in Figure 5, where the contribution percent of voltage is up to 61.21% for the electrodeposition of Ni, which is much higher than parameters, ca. the initial ion concentration, boric acid, and pH. Meanwhile, the voltage has a small influence (on the energy consumption, with only a 6.82% contribution [68].

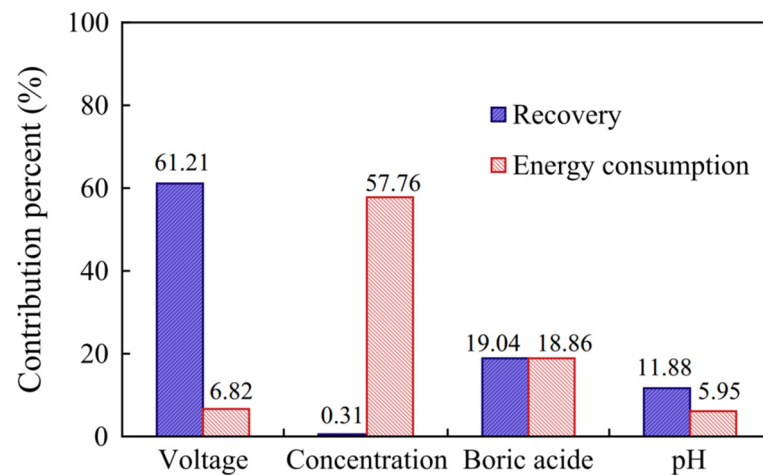


**Figure 5.** The contribution percent of the parameters (voltage, concentration, boric acid, and pH) of electrodeposition on Ni recovery and energy consumption. Reproduced with permission [68]. Copyright 2014, Elsevier.

However, optimizing other parameters such as pH, initial concentration, or flow rate is needed to maximize recovery efficiencies when using relatively lower voltage. For instance, the  $\text{Cu}^{2+}$  recovery efficiency could be increased from ~85% to ~95% at a constant voltage of 3.6 V when the pH was adjusted from 8.0 to 2.5, which is comparable to the recovery efficiency (~97%) at under 4.8 V with the pH value of 8 [69]. This can be attributed to the fact that a low pH environment can enhance the ion transport efficiency with low ohmic resistance and that it is beneficial to reduce the copper species into metallic  $\text{Cu}^0$ . This was further confirmed by X-ray photoelectron spectroscopy (XPS) analysis [69].

#### 4.2. Pulsed Current/Voltage Electrodeposition

In pulsed current/voltage electrodeposition, the current or potential changes periodically, respectively. It generates a constant current or voltage during the on-time ( $T_{\text{on}}$ ) pulse, which is followed by a pause when switched to the off-time ( $T_{\text{off}}$ ) pulse. Figure 6 shows the typical pulse-current waveform in the case of a pulsed current electrodeposition [70].

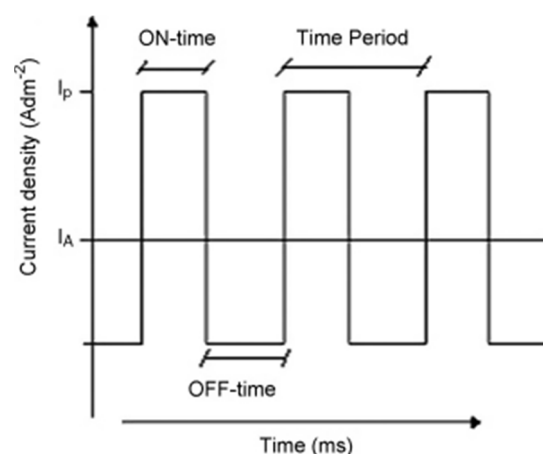


**Figure 6.** The typical pulse-current waveform showing  $T_{\text{on}}$  and  $T_{\text{off}}$  for one cycle. Reproduced with permission [70]. Copyright 2008, Elsevier.

For any given electrolyte, the peak current/voltage and the on-time and off-time pulses are the most important parameters to optimize to control the structure of the deposits [71]. Compared to conventional DC electrodeposition,  $T_{\text{off}}$  brings the biggest advantage to pulsed electrodeposition toward complete deposition, as it creates extra

time to fill the depletion region with additional metal ions at the electrode surface [72]. Moreover, due to the presence of  $T_{off}$ , the pulsed electrodeposition favours the initial growth of metal nuclei, increases the nuclei population density, and reduces their sizes distribution resulting in a fine grained deposit with uniformly small crystals [70]. The pulsed current electrodeposition can, for example, be used to obtain ultrafine zinc powders with the high recovery efficiency (88–92%) by optimizing the  $T_{on}$  and  $T_{off}$  parameters [73]. Moreover, the pulsed electrodeposition is suitable for recycling valuable metals occurring in low concentration. Hence, it was reported that, in combination with the pulsed current method and the static cylindrical electrodes, most of the silver in electroplating wastewater could successfully be recovered (>99%). Meanwhile, more than 95% of the present cyanide could be removed via the electro-oxidation process at the anode [72,74]. It is also worth noting that the total energy consumption of the pulsed electrodeposition is lower than when using conventional DC methods.

#### 4.3. Electrowinning and Electrorefining

Electrodeposition is the fundamental process for electrowinning and electrorefining during metal recovery. In electrowinning, a direct current is applied between the anode and cathode electrodes so that the targeted metal species can be reduced at the cathode and extracted in their metallic form [75]. During this process, some electrochemical oxidation reactions can simultaneously happen at the anode, which usually comprises of the oxygen evolution reaction ( $2\text{H}_2\text{O} = \text{O}_2 + 4\text{H}^+ + 4\text{e}^-$ ) [16].

Figure 7 shows a schematic description of electrowinning (A), including its current density–cell voltage dependence (B). It should be noted that the polarizations of these cathodic and anodic reactions have a significant influence on electrowinning's total energy consumption. Hence, a previous study revealed that the oxygen evolution reaction, in the case of industrial Cu electrowinning recovery, accounts for up to 70% of the total energy consumption [76]. Meanwhile, the concentration of metallic ion in solution gradually decreases as the electrowinning reaction progresses, which reduces current efficiency and increases the energy consumption. Thus, reducing the polarization of the involved reactions has been widely studied for industrial electrowinning.

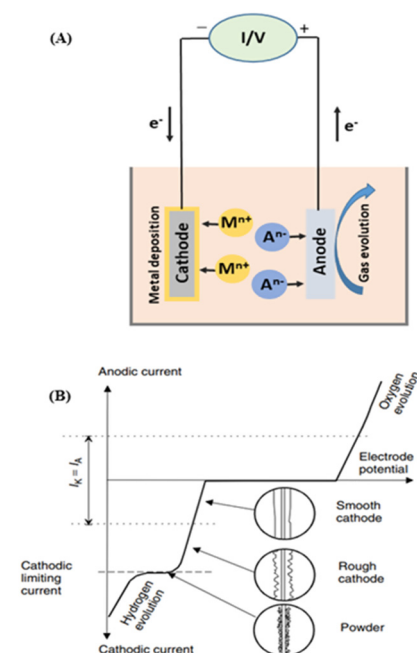


**Figure 7.** Schematic description of electrowinning process (A) and current density–cell voltage dependence for the electrowinning of copper (B). Reproduced with permission [16]. Copyright 2007, Wiley.

To that effect, it has been reported that the addition of  $\text{Fe}^{2+}$  ions can largely reduce the energy consumption needed for copper recovery from wastewater when compared to that without any  $\text{Fe}^{2+}$  ions [75]. A further study indicated that iron oxidation occurs at the anode instead of the oxygen evolution at the anode, thus strongly decreasing the cell voltage, ca. from 1.9 V to 0.7 V. Moreover, the authors applied a small potential to achieve selective Cu deposition through electrowinning. The latter process can also be used to efficiently recover bismuth (Bi) or antimony (Sb) with high purity (>95%) from spent electrolytes by using a cation exchange membrane [77,78].

Regarding electrorefining Figure 8 shows its schematic description (A) as well as its current density / cell voltage dependence (B). Electrorefining differs from electrowinning in that now the anode of the former consists of unrefined metals containing many impurities. During the electrorefining process, the anode gets partially dissolved into the solution via its direct or indirect electrooxidation, while some of these electroleached metal ions are selectively deposited into their pure forms onto the cathode [79]. Based on this principle, some electronic waste solids/powders can be packed together (for cohesion and electrical conductivity) and used as the anode where the base metals (e.g., Cu, Zn, Sn, Ni) are oxidized, and can then be electrowinned into their purified forms at the cathode. Meanwhile, remaining and unoxidized precious and/or rare earth metals are enriched in the anode material [80,81]. However, if too many different metals are involved, it creates numerous difficulties to enable a selective metal deposition at the cathode. For instance, since Mn is an active material exhibiting a fast dissolution during anodic oxidation, it is not suitable when mixed with copper for the latter conventional electrorefining. To address this issue, some authors proposed a method combining purification and electrorefining that enable the recovery of high purity Mn at the cathode [79]. To that end, an ion exchange is first performed that removes low concentration metals ions (Cu, Zn, Co, Cd, Ni) from the anolyte. It is then followed by Mn electrorefining at the cathode. As a result, the purity of the resulting Mn was in excess of 99.99%.

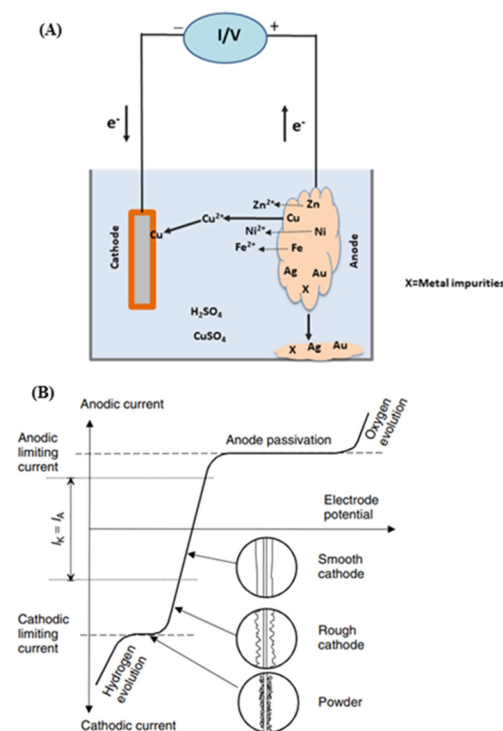


**Figure 8.** Schematic description of electrorefining process (A) and current density–cell voltage dependence for the electrorefining of copper (B). Reproduced with permission [16]. Copyright 2007, Wiley.

#### 4.4. Aqueous Electrolytes Based Electrochemical Methods

Aqueous solutions have been widely used as electrolytes for electrodeposition in the above studies, due to their ability to be more easily handled and deployed at the industrial scale. Nevertheless, several challenges still persist that need to be solved in order to further improve its selectivity and the associated metal recovery economic effectiveness. As previously mentioned, hydrogen evolution is the main side reaction during metal ion reduction at the cathode in aqueous electrolytes, which results in low current efficiency and high energy consumption [82]. To improve this efficiency, one must optimize the aforementioned operating parameters, including the initial metal concentration, the electrolyte composition, the pH, and so forth [67]. More recently, a sono-electrochemical strategy, which uses sound waves in conjunction with the electrochemical process, was proposed to efficiently recover valuable Pd, Pb, and Ga metals from their aqueous solutions [83]. When compared to the lone electrochemical process at constant voltage, the reduction ratio of the selected metals showed a significant increase with the assistance of ultrasounds, depending on the megasonic frequency that was used (shown in Figure 9). This may be ascribed to the increased temperature in a highly reduced environment under sonication. Indeed, the high-power density of sonicator can induce violent oscillations of the hydrogen bubbles surrounding the cathode, which then can generate a large number of hydrogen radicals as the temperature rises. Other effects could also play some role, such as accelerated mass transfers that can be both ion and frequency dependent [84].

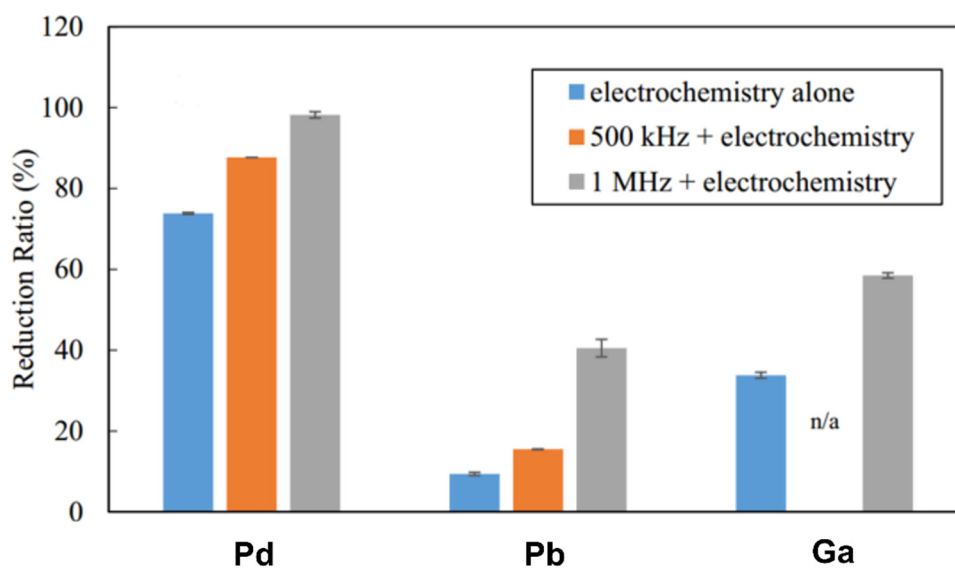


**Figure 9.** Reduction ratio of Pd<sup>2+</sup>, Pb<sup>2+</sup>, and Ga<sup>3+</sup> metal ions over 60 min in Ar-saturated solution (with or without 500 kHz or 1 MHz sonication). Reproduced with permission [83]. Copyright 2016, Elsevier.

Moreover, the selective recovery of metals from a solution containing complex mixtures of metal species (especially in the case of e-waste) is the most difficult problem to solve because of the M<sup>n+</sup>/M couples' close redox potentials values [85]. Thus, to ensure such desired selectivity and to obtain high purity metals, one of the more feasible strategies is first to remove some of the metal species from the considered complex solutions through chemical precipitation, solvent extraction, or ion exchange [79,86–88]. Interestingly, Mecucci and Scott used a combination of chemical leaching, precipitation and electrodeposition in order to selectively recover Sn, Cu, and Pb from scrap printed circuit boards (PCBs) [88]. First, nitric acid (HNO<sub>3</sub>) was used as the leaching reagent to dissolve Cu, Pb, and Sn from the PCBs. Sn was then precipitated in its H<sub>2</sub>SnO<sub>3</sub> solid form by using an initial concentration of HNO<sub>3</sub> greater than 4 mol L<sup>-1</sup>. NaOH was then added to neutralize the remaining HNO<sub>3</sub> and allow for a better electrodeposition. Finally, the residual Cu<sup>2+</sup> and Pb<sup>2+</sup> were deposited separately as metallic Cu and PbO<sub>2</sub>, onto the cathode and the

anode, respectively, by using a suitable applied potential (shown in Figure 10). Notably,  $\text{HNO}_3$  and  $\text{NaOH}$  can be regenerated due to the production of hydrogen and hydroxide ions during water splitting.

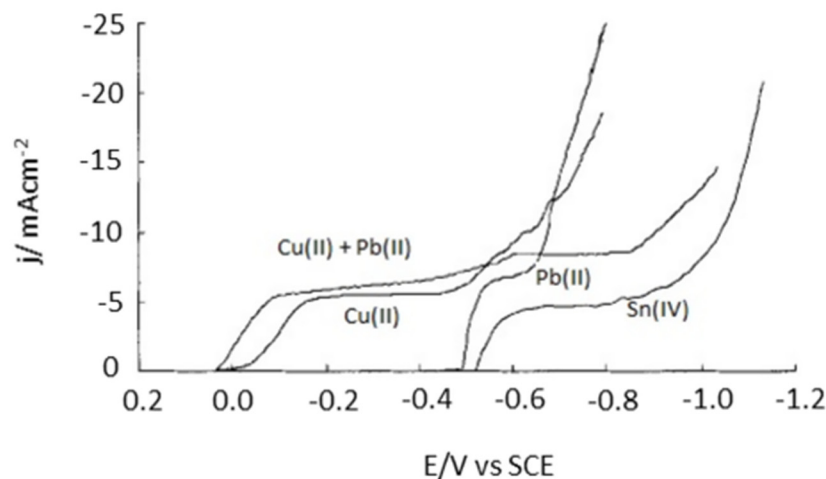


**Figure 10.** The LSV curves for 0.01 M  $\text{Cu}(\text{NO}_3)_2$  + 0.5 M  $\text{NaNO}_3$ , 0.01 M  $\text{Pb}(\text{NO}_3)_2$  + 0.5 M  $\text{NaNO}_3$ , 0.01 M  $\text{Cu}(\text{NO}_3)_2$  + 0.01 M  $\text{Pb}(\text{NO}_3)_2$  + 0.5 M  $\text{NaNO}_3$ , 0.01 M  $\text{H}_2\text{SnCl}_6$  + 1.5 M  $\text{HCl}$  at a scan rate of  $5 \text{ mV s}^{-1}$ . Reproduced with permission. [88] Copyright 2002, Wiley.

Even more advanced, a recent combined electroleaching/electrodeposition method has led to a significant improvement in efficient metal recovery. It consists of: (i) a selective electrooxidation to control the metal ion specie that is generated at the anode; (ii) the simultaneous electroreduction of the corresponding metal ion at the cathode [89]. It is worth noting that a separator between the anode and cathode is essential to control metal migration and to prevent the deposited metal layer from wearing off because of the anodic solids. Generally, anodic electroleaching can be completed by means of direct or indirect electrooxidation. In direct electrooxidation, the anode is composed of raw materials containing different metals to be oxidized directly without the help of additional leaching reagents [90,91]. For example, the direct electrooxidation method was used to selectively leach Sn and Pb from a waste solder alloy under optimised conditions ( $0.5 \text{ M H}_2\text{SO}_4$ ,  $60 \text{ A m}^{-2}$  and flow rate of  $45 \text{ mL min}^{-1}$ ). In this method, up to 82 wt% Pb was recovered as  $\text{PbSO}_4$  ( $\text{Pb} + \text{SO}_4^{2-} \rightarrow \text{PbSO}_4 + 2\text{e}^-$ ) at the anode, and the  $\text{Sn}^{2+}$  that had leached from the waste solder was reduced into its pure metal form onto the cathode ( $\text{Sn}^{2+} + 2\text{e}^- \rightarrow \text{Sn}$ ) [90]. If one now deals with Copper (Cu) and antimony (Sb), that can be recovered from e-waste (RAM memory and integrated chips circuits, their recovery involves a leaching step in a solution of  $0.5 \text{ mol dm}^{-3}$  hydrochloric acid (HCl) and  $0.074 \text{ mol dm}^{-3}$  ferric chloride ( $\text{FeCl}_3$ ) at a 1:10 solid/liquid ( $w/v$ ) ratio followed by an electrodeposition in an aqueous solvent. Under these conditions, 96 wt% of the copper was electrochemically recovered from the leachate solution [23]. Antimony could also be recovered from the leachate solution as an antimony precipitate (81 wt% in purity) through pH modification (by adding NaOH pellets).

In contrast, indirect electrooxidation is a process used to perform selective anodic metal leaching using in situ generated oxidants (e.g.,  $\text{Cl}_2$ ,  $\text{H}^+$ ,  $\text{Fe}^{3+}$ ). Hence, some authors conducted the indirect electrooxidation process with an  $\text{Fe}^{3+}/\text{Fe}^{2+}$  redox couple to selectively recover high-purity Cu (99.9%) from waste PCBs while precious metals (Au and Ag) were enriched in the anodic sludge [92]. Considering the factors of current efficiency, deposit composition, and energy consumption, they optimized the flow rate to  $400 \text{ mL/min}$ , therefore, achieving 75% metal extraction from waste PCBs.

Alternatively, a one-step slurry electrolysis was used, combining the in situ metal leaching from CPU sockets using the mixed  $\text{HCl-NaCl-H}_2\text{O}_2$  system. This resulted in the enrichment of Au species in the electrolyte, as well as high purity Cu to electrodeposit at the cathode (Figure 11) [19,81]. By optimizing the operating conditions ( $4 \text{ M HCl}$ ,  $75 \text{ g L}^{-1}$

pulp density and  $80 \text{ mA cm}^{-2}$  for 4 h), they achieved a Cu recovery efficiency of 96.67% with high Cu purity (98.16 wt%). Similarly, the Au recovery efficiency reached 95.73% under the following optimised conditions: 4 M HCl,  $100 \text{ g L}^{-1}$  pulp density,  $70 \text{ mA cm}^{-2}$  for 4 h). In short, we believe that this combination of electroleaching and electrodeposition is one of the most promising directions for future research, because: (i) it enables an efficient and selective recovery of high purity valuable metals from complex system, and; (ii) its scale up toward industrial capacity showed promising insights.

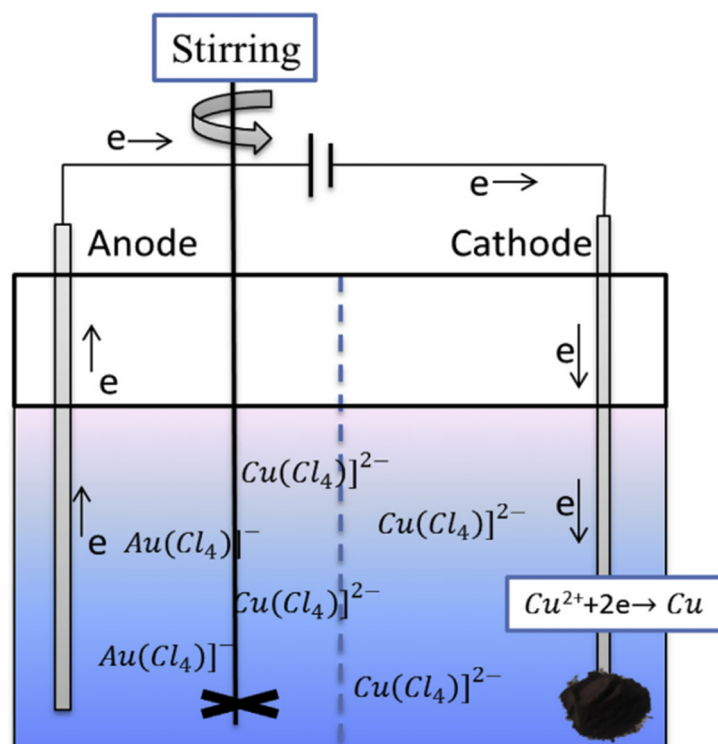


**Figure 11.** Schematic diagram of the electrodeposition process in HCl-NaCl-H<sub>2</sub>O<sub>2</sub> system. Reproduced with permission [81]. Copyright 2019, Elsevier.

#### 4.5. Non-Aqueous Electrolytes Based Electrochemical Methods

When compared to aqueous electrolytes, metal recovery through electrodeposition from non-aqueous electrolytes has shown the unparalleled advantages of wide electrochemical windows and high stability. Such non-aqueous electrolytes include conventional organic solvent (e.g., dimethylsulfoxide, dimethylformamide), molten salts (e.g., LiCl-KCl, LiF-CaF<sub>2</sub>), ionic liquids [93,94], and deep eutectic solvents (DESs) [95–97]. If one except the classical organic solvents, other non-aqueous electrolytes are usually costly as they are custom made and must be synthesized in their pure form. However, despite purification efforts, these solvents often come with impurities, resulting of the multi-step synthetic and purification process steps. The presence of such metal ions impurities may affect the electrodeposition of targeted metal ions in a regressive way. In this section, special attention will be paid to ionic liquids and deep eutectic solvents, which hold wider application prospects because of their unique set of favorable properties, when compared to other media, such as low melting temperature, non-volatility, and high thermal stability [98]. Accordingly, their use has resulted in the cathodic deposits of precious metals (e.g., Pt, Pd, Rh), rare earth elements, and other metals (e.g., Ta, Zr, Gd) that cannot be achieved through electrolysis in aqueous solutions [28]. Notably, an ionic liquid system (n-hexyl-trimethyl ammonium bis(trifluoromethyl-sulfonyl)amide, [N1116][TFSA] and tri-n-butylphosphate, TBP) was used to extract indium (In) from used liquid crystal displays (LCDs) followed by direct potential controlled electrodeposition for the recovery of In metal [93]. Electrochemical quartz crystal microbalance (EQCM) analyses indicated the formation of an In deposit

on the cathode at  $-0.81$  V (vs.  $\text{Fc}/\text{Fc}^+$ ) via a single-step three-electron reduction process. The authors also reported combined electroleaching and electrodeposition processes in ionic liquids to selectively recover high purity Pt from used membrane electrode assemblies (MEA) from proton exchange membrane fuel cells (PEMFCs) [89].

In another report, using the selected 1-butyl-3-methyl imidazolium chloride (BMIM Cl)/1-butyl-3-methyl imidazolium bis(trifluoromethylsulfonyl)imide (BMIM TFSI) system, a Faradaic yield of up to 100% was obtained with a leaching rate of  $3.3 \text{ mg}\cdot\text{h}^{-1}\cdot\text{cm}^{-2}$  (which is comparable to the leaching rate of  $4.0 \text{ mg}\cdot\text{h}^{-1}\cdot\text{cm}^{-2}$  in aqua regia) for a cathodic Pt deposition at  $-1.3$  V (vs.  $\text{Ag}^+/\text{Ag}$ ). This occurred without any electrolyte degradation (shown in Figure 12). Moreover, even various ionic liquids such as (1-butyl-3-methylimidazolium chloride salt), (1-butyl-3-methylimidazole tetrafluoroborate), (1-ethyl-3-methylimidazole chloride), and (1-butyl-3-methylimidazolium hexafluorophosphate) have been used in combination with an additive agent (NaCl) and an oxidising agent  $\text{H}_2\text{O}_2$  in order to leach copper from e-waste PCBs [99].

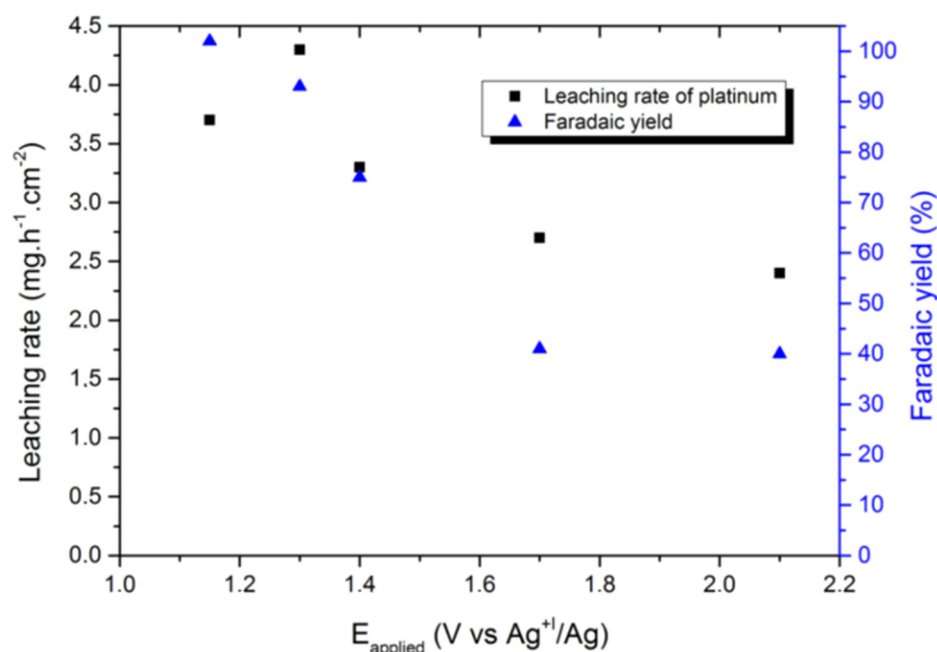


**Figure 12.** Effect of the applied potential on the leaching rate of platinum and the corresponding Faradaic yield in runs conducted at  $Q = 55 \text{ C}\cdot\text{cm}^{-2}$ . Reproduced with permission [89]. Copyright 2018, Creative Commons.

For copper, the ionic liquid-based electrolyte solution of  $\text{CuSO}_4 - \text{NaCl} - \text{H}_2\text{SO}_4 - [(1\text{-butyl-3-methylimidazolium hexafluorophosphate})]$  has been reported for its recovery with a good yield (92.65 wt%) through slurry electrolysis using graphite and titanium as positive and negative plates, respectively.

Regarding the electrodeposition in deep eutectic solvents, they can exhibit significantly different properties in comparison to those obtained when using aqueous solutions. Indeed, it was reported that the deposition rates of nickel in aqueous and deep eutectic solvents are similar (despite the differences in the viscosity and the conductivity of these two systems), the nickel deposits from deep eutectic solvents was more prone to form nanocrystals having lower surface roughness and higher hardness than the microcrystals obtained using aqueous solutions [97].

In the case of batteries, a recent work combining both IL and DES allowed for the better separation of all of the metallic elements involved [100]. First a liquid–liquid extraction step was reported using  $N,N,N',N'$ -Tetra-*n*-octyldiglycolamide (TODGA) as an extractant dissolved in 1-butyl-3-methylimidazolium bis(trifluoromethylsulfonyl)imide. A 99% total of manganese could be recovered in this single step. Cobalt recovery (90%) was then

performed using tri-hexyltetradecylphosphonium chloride. Finally, for the recovery of nickel and lithium, DES based on lidocaine and carboxylic acid was used to allow the retention of lithium in the solution and the extraction of nickel. However, the exploration of electrodeposition in ionic liquids or deep eutectic solvents is still in its infancy. Several key issues that impede the practical applications of these solvents have yet to be solved, hence representing promising fields of future research. First, the physical and chemical properties of these liquids might change when they are exposed to moisture for a long time [101]. Moreover, the electrochemical behavior of metals in ionic liquids and DES remains poorly understood in published works. Furthermore, there is still a lack of knowledge on their environmental impact. Finally, their cost of can be much higher than that of an aqueous electrolyte.

If one now considers molten salts, the rare earth element neodymium (Nd) can electrochemically be recovered from NdFeB magnets using molten salt electrolysis [102]. During the process, the solid NdFeB material is directly placed in an anodic compartment with molten fluorinating agents (e.g.,  $\text{AlF}_3$ ,  $\text{ZnF}_2$ ,  $\text{FeF}_3$  and  $\text{Na}_3\text{AlF}_6$ ), which converts Nd from a the magnetic alloy into  $\text{NdF}_3$  salt melt [103,104]. The  $\text{Nd}^{3+}$  ions from the molten salt can then be electrodeposited at the cathode. Additionally, the rare earth elements Nd and Pr, which can also be found in permanent magnets, can successfully be recovered through an electrorefining process in molten fluorides [105]. Figure 13 shows the composition of the cathodic deposits and the current efficiency as a function of the applied currents. With an increase in the applied current, the Nd and Pr content shows almost no change, but the Fe content increased rapidly. In this electrorefining process, a permanent magnet is selectively oxidized and is dissolved into molten  $\text{LiF-CaF}_2$  salts, and the free rare earth ions are directly reduced into their metallic form at the cathode. The molten salt electrolyte-based electrochemical recovery eliminates the additional oxide or halide conversion steps of the hydrometallurgical processes. Table 3 summarizes metal recovery from e-waste using electrochemical approaches, electrodeposition, and electrowinning.

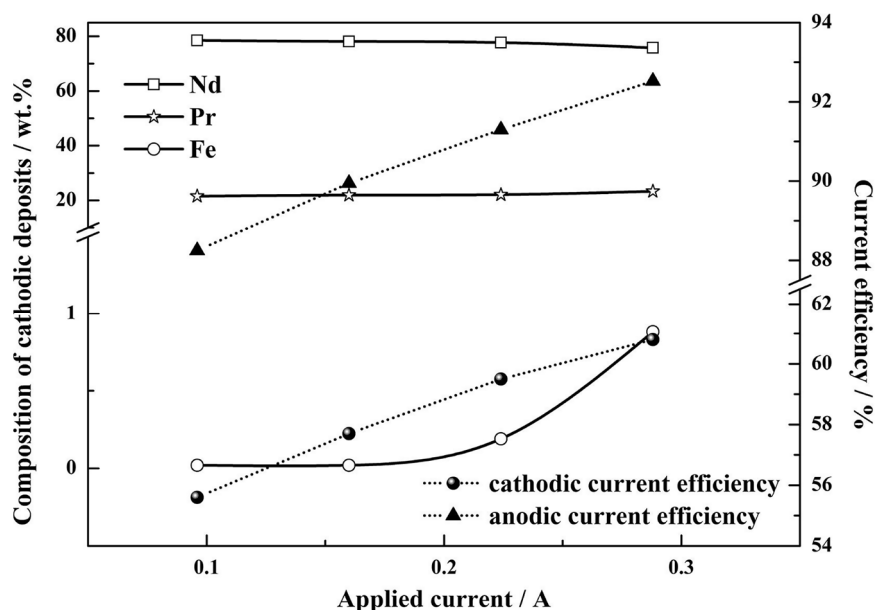


Figure 13. The composition of cathodic deposits and current efficiency as a function of applied currents. Reproduced with permission [105]. Copyright 2020, Elsevier.

**Table 3.** Summary of metal recovery from e-waste using electrochemical approaches, electrodeposition, and electrowinning.

Target Metals for Recovery from E-Waste/Leachates/Feeds	Electrolyte Used in Electrochemical Approaches	Metal Purity % and (Recovery %)	Operating Parameters	Ref.
Cu <sup>2+</sup> and Pd <sup>2+</sup> ions from e-waste MLCCs	HNO <sub>3</sub>	Pd purity >99% and recovery 99.02%	−0.25 V, agitation speed of 240 rpm and 0.5 M HNO <sub>3</sub>	[62]
Fe <sup>2+</sup> and REE ions from permanent waste magnets (Nd-Fe-B)	(NH <sub>4</sub> ) <sub>2</sub> SO <sub>4</sub> and (Na <sub>3</sub> Citrate)	REEs recovery (93.7% Nd, 3.1% Dy and 2.6% Pr) with high purity of 99.4%	pH value of 3.5~4.5, current density of 25 mA cm <sup>−2</sup> at the anode	[65]
Zn <sup>2+</sup> , Cu <sup>2+</sup> , and various metal ions from flue dusts	NaOH	Recovery of 88–92% of Zn	Pulse current electrolysis at T <sub>on</sub> = 15 ms and T <sub>off</sub> = 10 ms	[73]
Low concentrated Ag <sup>+</sup> ions in electroplating wastewater	Silver electroplating rinse			
Wastewater (200 ± 10.0 mg L <sup>−1</sup> and 150 ± 10.0 mg L <sup>−1</sup> cyanide at pH 10.0 ± 0.5)	NaCl addition of 0.05 mol L <sup>−1</sup> at room temperature	99% of Ag	Voltage (4.0 V), frequency (800 Hz), duty cycle (50%) pH 9.5 ± 0.5, aeration rate of 100 L h <sup>−1</sup> , and stirring speed of 1000 rpm with	[72]
Spent electrolytes with Bi, Sb, and Cu ions	Catholyte: NaCl and H <sub>2</sub> SO <sub>4</sub> for Bi, HCl for Sb Anolyte: H <sub>2</sub> SO <sub>4</sub>	Bi 97% and Sb 96% purity	−0.1 V and −0.25 V (vs. Ag/AgCl) at 10 mA cm <sup>−2</sup> for Bi and Sb, respectively.	[77]
Nd, Pr, and Fe components from rare-earth permanent magnet (REPM) wastes	Molten LiF-CaF <sub>2</sub> salts	~80% and ~20% purity of Nd and Pr, respectively. Fe impurity increases from 0 to 1% with the increase of applied current (0.1–0.3 A)	REE elements were directly reduced into metallic form at cathode.	[105]
Electrowinning of Cu <sup>2+</sup>	Ammonical alkaline solutions containing Cu(I) ions and an ammonium salt of sulfate or chloride or nitrate		The cathode current efficiency during the copper electrodeposition ~90% for chloride, ~80% for sulfate, and ~30% for nitrate salt electrolyte	[82]
Sonoelectrochemical recovery of Pd <sup>2+</sup> , Pb <sup>2+</sup> , and Ga <sup>3+</sup>	Pd(NO <sub>3</sub> ) <sub>2</sub> -HNO <sub>3</sub> electrolyte for Pd	~100% palladium reduction ratio at condition of 120 min with acoustic field of 1 MHz sonication	+0.987 V vs. Ag/AgCl (sat. KCl) for Pd <sup>2+</sup> reduction using Pt mesh as working electrode and counter electrode	[83]
	PbCl <sub>2</sub> -CH <sub>3</sub> COONH <sub>4</sub> electrolyte for lead	~60% lead reduction ratio at condition of 120 min with acoustic field of 1 MHz sonication	0.126 V vs. Ag/AgCl (sat. KCl) for Pb <sup>2+</sup> reduction using copper sheet as working electrode and Pt mesh counter electrode	
	GaCl <sub>3</sub> -NaCl electrolyte for gallium.	~75% gallium reduction ratio at condition of 120 min with acoustic field of 1 MHz sonication	−0.530 V vs. Ag/AgCl (sat. KCl) for Ga <sup>3+</sup> reduction using vitreous carbon rod as working electrode and Pt mesh counter electrode,	
Sn and Pb recovery from waste solder alloy	(0.5 M H <sub>2</sub> SO <sub>4</sub> , 60 A m <sup>−2</sup> and flow rate of 45 mL min <sup>−1</sup> )	82 wt% Pb is recovered as PbSO <sub>4</sub> at the anode; Sn is recovered as cathodic deposit		[90]

Table 3. Cont.

Target Metals for Recovery from E-Waste/Leachates/Feeds	Electrolyte Used in Electrochemical Approaches	Metal Purity % and (Recovery %)	Operating Parameters	Ref.
Cu and Au recovery from CPU sockets	Electroleaching/electrodeposition	Cu recovery efficiency of 96.67% with high Cu purity (98.16%); Au recovery efficiency 95.73%	Operating conditions (4 M HCl, 75 g L <sup>-1</sup> pulp density, 80 mA cm <sup>-2</sup> and 4 h) for Cu and (4 M HCl, 100 g L <sup>-1</sup> pulp density, 70 mA cm <sup>-2</sup> and 4 h) for Au.	[81]
Selective In recovery from spent LCDs using ionic liquid extraction and electrodeposition	[N <sub>1116</sub> ][TFSA] and [TBP]	In 81.46 wt%, Ni 3.34 wt%, Zn 15.20 wt%	Potentiostatic electrodeposition of extracted [In(TBP) <sub>3</sub> <sup>3+</sup> ] in [N <sub>1116</sub> ][TFSA] at -1.0 V on a platinum quartz crystal electrode, Overpotential E/V vs. Pt QRE	[93]
Pt recovery from spent membrane electrode assemblies	(BMIM Cl)/(BMIM TFSI) system	-	Pt deposition at -1.3 V (vs. Ag <sup>+</sup> /Ag)	[89]

#### 4.6. Electrodeposition in Supercritical Fluids

Pushed by the unique properties of supercritical fluids (SCFs), such as tunability, low viscosity, enhanced mass transport, lack of surface tension, and simple separation of reagents and products, electrochemistry in SCFs has gained an ever increasing attention over the past forty years [106–110]. Bartlett and co-workers published a comprehensive review in 2014 elaborating on both the practical and scientific aspects of electrodeposition in supercritical fluids (SCFED), where various metals of interest for e-wastes like Cu, Ag, and Ge were covered [111]. A range of different substances have been used as SCFs for electrodeposition, including carbon dioxide (CO<sub>2</sub>), water (H<sub>2</sub>O), ammonia (NH<sub>3</sub>), and more recently, Argon (Ar) or hydrofluorocarbons (HFCs), some of which have accessible critical conditions and large deposition windows [112]. However, the key challenges of such electrodeposition approaches along with their significant advantages lie in the complications arising from pressurized reactor designs, difficulties due to the removal or replacement of electrodes as well as low dielectric constants and the poor solubility of ionic species for some SCFs [109,113]. To the best of our knowledge, SCFED has not yet been implemented as an industrial process by the e-waste recycling industry. Therefore, we focus here on the most recent advance in the field of SCFED since 2015 in order to anticipate their possible applications for metal recovery from e-waste.

For SCFED studies, supercritical CO<sub>2</sub> (ScCO<sub>2</sub>) is not ideal as a non-aqueous medium because of its low dielectric constant ( $\epsilon < 1.8$ ), thus leading to the low solubility and dissociation of ionic species and its resulting low conductivity [114]. To overcome this issue, some approaches were proposed that primarily concerned the implementation of microelectrode systems, the use of highly hydrophobic supporting electrolytes, and the addition of polar co-solvents [109]. The latter two approaches, so-called modified single-phase ScCO<sub>2</sub>, are preferred, especially for larger scale production [110]. Pt electrodeposition was studied using dimethyl(1,5-cyclooctadiene)platinum as a precursor from a ScCO<sub>2</sub>-based electrolyte with the addition of acetonitrile (co-solvent) and tetrabutylammonium tetrafluoroborate (supporting electrolytes) [115]. The authors demonstrated that platinum was potentiostatically electrodeposited with the formation of the agglomerates being made of densely packed nanoparticles [115]. Furthermore, the successful electrodepositions of copper and silver using a similar SCFED technique have also been reported [116,117].

HFCs are however more useful for SCFED media thanks to their accessible critical conditions, more polar nature, and higher dielectric constant, so that the addition of a polar co-solvent is not necessarily needed [110]. Champion et al. synthesized some hexahalide salts that incorporated trivalent metal ions from group 3 as well as lanthanides and showed their enhanced dissociation in HFCs solvents [118]. A variety of supporting electrolytes were reported, such as  $[N(nC_4H_9)_4][Al(OC(CF_3)_3)_4]$ ,  $[N(nC_4H_9)_4][FAP]$ , and  $[N(CH_3)_4][FAP]$  ( $[FAP]^-$  tris(pentafluoroethyl)trifluorophosphate), which not only provide high electrical conductivity in supercritical  $CH_2F_2$  but also meet the requirements imposed by different precursors and process parameters [119]. Bartlett et al. reported a common approach to the SCFED for a range of p-block elements from supercritical  $CH_2F_2$  in the presence of tetrabutylammonium chloride as the electrolyte [120]. With anionic and dianionic chlorometallate salts, the deposition of elemental Ga, In, Ge, Sn, Sb, Bi, Se, and Te was demonstrated [120]. The electrodeposition of protocrystalline Ge films onto TiN electrodes with  $[GeI_3]^-$  as precursor was also reported by analogous means [121]. When templates such as metal coated anodic aluminium oxide membranes were used for SCFED, tellurium [122] and tin nanowires [123,124] were fabricated with a high-quality crystalline structure.

Although more and more of the valuable metals that can be found in e-waste have now been verified to electrodeposit in SCFs, the precursors used in these SCFED experiments were all pure and handpicked reagents that met several stringent criteria, including good solubility and stability in low-polarity SCFs, electrodeposition at accessible potentials, exemption from undesirable electrochemistry, or fouling at the counter electrode [111]. Hence, regarding real life leachates from e-waste processing, the challenge of conversion from a miscellaneous metallic solution to highly effective reagents for SCFED must be investigated. Once this is solved, we believe that the combination of SCFED with e-waste recycling can have a promising future, not only because it provides a more environmentally friendly approach to metal recovery from e-waste without generating acidic electrolyte effluent, but also because it permits the synthesis of value-added nano-structured electrodeposits that can find potential usage for microelectronic components, optical and catalytic applications, chemical and biochemical sensors, etc. [123,125–128].

#### 4.7. Electroplating with the Aid of Supercritical Fluids

Compared to conventional electroplating, electroplating in SCFs (SCFEP) can offer additional advantages including a lack of hydrogen production, grain refinement, higher coating hardness, shorter fabrication times, and better coverage [129]. Unlike SCFED conducted in a single SCF phase, SCFEP was normally studied in emulsified SCFs consisting of an aqueous electrolyte and a SCF. With the aid of a small amount of surfactant, Au film [129], Co film [130], Co-Ni alloy coating [131], Cu-Ni alloy coating [132], and Ni-SiC nanocomposites [131] were fabricated in emulsified  $ScCO_2$  baths, and they all displayed smaller grain sizes, smoother surfaces, and enhanced mechanical properties. Furthermore, the use of ultrasound was reported to replace the role of the surfactant in electroplating processes, and the resulting Cu film [133], Ni coating [134], Ni-Co alloy coating [135], and Ni-Co-P alloy film [136] all exhibited superior tribological and anti-corrosive properties to those same materials that had been fabricated using either a regular  $ScCO_2$  or a conventional method. However, some undesired by-products, such as carbonic acid, are inevitably produced in emulsified  $ScCO_2$ , so noble gases (e.g., Ar) were tested for ultrasound-assisted SCFEP, and the resulting Cu films had finer grains, a better aesthetic finish, and enhanced mechanical and corrosion behavior [137,138]. It can thus be inferred that one can take advantage of SCFEP to recover metals and fabricate metal or alloy coatings from e-waste leachates as long as a proper conversion of the leachates can be achieved. Table 4 summarizes the advantages and disadvantages of electrochemical processes during metal recovery.

**Table 4.** Advantages and disadvantages of electrochemical processes during metal recovery.

S.N.	Electrochemical Processes	Advantages	Disadvantages
1	Potential controlled electrodeposition	Highly selective metal recovery	Thickness non-uniformity
2	Current controlled electrodeposition	Electrocrystallization to obtain large crystals	Thickness non-uniformity, co-deposition of different metal species
3	Pulsed current electrodeposition [70]	Fine control on electrodeposit structure	Pulse rectifier costly
4	Pulsed voltage electrodeposition [70]	Fine control on electrodeposit structure	Pulse rectifier costly
5	Electrowinning and electrorefining	Large areas and thicker deposition	Hydrogen embrittlement, hydrogen evolution
6	Aqueous electrolyte-based	Inexpensive and plenty	Hydrogen embrittlement, hydrogen evolution
7	Non-Aqueous electrolyte-based	Large window stability, selective deposition	Costly and metal ions impurities
8	Supercritical fluid-based electrodeposition	Tunability, enhanced mass transport and selectivity	Pressurized reactor designs

## 5. Industrial Perspective

Electrodeposition-based metal recovery can lead to selective metal reduction and deposition. However, this is hindered by the multi-metal nature of leachate solutions obtained from e-waste, which leads to the co-deposition of other metals along with the targeted one. Hence, to achieve high purity metal recovery, it is required to perform selective metal leaching using selective lixivants. Such leachate, containing only targeted metals, can be obtained following efficient sorting and physical separation process steps followed by one or more selective leaching steps. Moreover, further leachate processing is required in case of non-selective leaching, where multiple metal ions are dissolved and collected in the same leachate solution, in order to improve purity in subsequent recovery processes.

To demonstrate the economic feasibility, Lister et al. (2016) provided a technical-economic comparison of electrochemical recovery (ER) and hydrometallurgical processes from the point of view of capital equipment (CAPEX) and operating expenditures (OPEX) [139]. The estimated CAPEX for ER process was USD 405.98 per ton of e-waste, which was lower than the USD 653.46/ton of hydrometallurgical processes. Furthermore their study showed that the OPEX of the ER process is low since the electrolytes can be regenerated and kept within the cycle loop, and the largest OPEX contribution comes from the e-waste feedstock. Thus, it is very important to develop more efficient e-waste collection strategies to further improve its economic viability. Furthermore, other methods such as life cycle and Biwer–Heinzle analyses have been developed to assess environmental impacts. For example, on the basis of a tool for the reduction and assessment of chemical and environmental impacts (TRCI) and for international reference life cycle data (ILCD), Li et al. (2019) conducted a comparative life cycle analysis to give quantitative insight into the environmental performance of the pyrometallurgical, hydrometallurgical, and ER processes used for the precious metal recovery from e-waste [19]. Their results showed that the ER process outperforms the other two processes with reduced environmental impact. Indeed, with most of the oxidants used in electrolytes for the ER process that can be effectively recycled, the main environmental impact contributors are the hydrochloric acid, the hydrogen peroxide, and the sulfuric acid inputs.

Some other challenges however remain for electrochemical processes that impede its large-scale and industrial application in metal recovery, such as the low current densities or efficiencies of metal electrodeposition and poor selectivity in the case of complex leaching solutions [83,89]. Moreover, some toxic products (e.g., Cl<sub>2</sub>, NO<sub>x</sub>) may be generated in some specific electrolyte systems and conditions. It is not only difficult to control the

environmental impacts associated with the electrodeposition process, but the metallic deposits can also be redissolved because of the strong oxidizing nature of the toxic products generated at the anode [89,140]. To address this issue, it is highly desirable to develop either less hazardous and regenerable electrolyte systems instead of hazardous  $\text{Cl}^-$  and  $\text{NO}_3^-$  containing reagents or new strategies for preventing the evolution of toxic products. For instance, cation exchange membranes can be used to prevent chloride migration from the cathodic chamber to the anodic one [77]. Moreover, electrodeposition from a dilute metallic solution also suffered from seriously low current efficiency, which leads to a limited mass transfer accompanied by numerous side reactions, especially in high acidic systems. In this regard, a proper electrochemical cell design with a high electrode surface area, a fast electrolyte flow rate or with an electrode movement is essential to facilitate mass transfers during electrodeposition. Recently, a tubular EMEW<sup>®</sup> cell was employed to enable a selective and efficient recovery of low concentrated copper and tellurium ions from a HCl leaching solution [3]. Therefore, a significant amount of future research in this field should be devoted to eliminating these limitations and to optimizing the ER process.

Finally, leaching chemical(s) and electrolytes must be chosen carefully. For example, leachates from e-waste contain metal ions dissolved in either an acidic or basic solution, which later require treatments that can negatively affect OPEX. Additionally, precious metals, e.g., gold or silver, are often present in leachate solutions as soluble metal cyanide coordination complexes. Hence, highly toxic electrolyte systems comprising  $\text{CN}^-$  create an environmental burden and severe health hazards to human being and can be the cause of major OPEX contributions or liabilities. Therefore, an electrolyte system should be selected to be as safe as possible while also not increasing the associated OPEX (nor CAPEX).

The limitations of electrochemical processes should be addressed before translating metal recovery using electrodeposition to an industrial scale. Indeed, metal recovery from e-waste is quite expensive, especially when strictly following environmentally conducive requirements, including using less hazardous and less toxic chemicals. Therefore, e-waste recycling processes should be economically viable for their widespread implementation. Industrial facilities for metal recovery from e-waste should adopt integrated combined pyro-, hydro-, and electrometallurgical processes. There are only a few important industrial facilities that recover metals from e-waste: (i) Umicore, which is an integrated smelting and refining facility; (ii) the Noranda process in Quebec; (iii) Rönnskär's smelters in Sweden; (iv) Kosaka's recycling plant in Japan; (v) the Kayser recycling system in Austria; (vi) the Metallo-Chimique N.V plants in Belgium and Spain; and (vii) the Solvay hydrometallurgy plant in La Rochelle [141]. Often, these processes are made to be economically viable because the CAPEX was able to be reduced thanks to the reuse or the conversion of an already depreciated plant or facility. It is worth mentioning that most of such industrial facilities, except Solvay's, recover base metals (Cu, Zn, Sn, Ni), precious metals (Au, Ag, Pd, Pt, Ir, Ru, Rh), and critical elements (In, Ga), but the extraction of rare earth metals still remains challenging, possibly due to their relatively lower amounts or concentration in waste and further loss of rare earth metals in the separation and pre-treatment steps. Therefore, developing efficient rare earth metals recovery processes that are viable for industrial facilities represent an important and necessary goal to achieve while also considering their strategic and commercial relevancies.

## 6. Conclusions

Electrochemical processes-based metal recovery from e-waste use much less solvent (minimal reagent) and show convenient and precise control, reduced energy consumption, and low environmental impact. Since the total amounts of metal constitute up to 40 wt% in e-waste (in the case of PCB) with the goal to minimize waste, it is ideally necessary to fully and efficiently recover copper, aluminium, ferrous, precious and critical metals (including rare earth elements) in an economically viable way. These metals are, however, present in very different concentrations with, for example, copper that is found in e-waste in concentrations up to 10–27 wt%, precious metals in concentrations of less than 1 wt%, and

rare earth metals at even smaller amounts. Hence, although the recovery of precious metals and rare earth metals is critical due to their strategic importance and intrinsic value, their dispersion and overall small concentrations in e-waste represent a phenomenal challenge to render any recovery process economically viable. Therefore, metal profiling in e-waste is key to assure a balanced spreadsheet after recovery and recycling, and thus for each new e-waste batch received.

Since leachates from e-waste usually contain multiple dissolved metals ions with similar physical and chemical properties, they may lead to purification difficulties during metal recovery and additional OPEX. Furthermore, one must not overlook the high variability in the composition of e-waste when going from one lot to another. Electrochemical methods such as electrodeposition and electrowinning bring possible responses to the selective recovery of metal ions from leachate with multiple ions at a selected applied potential, as it relies on redox potential of metal ions for reduction—electrodeposition. The limiting aspects of these electrochemical methods are the adsorption of non-electroactive species on the electrode from the electrolytes, non-uniform potential, and inhomogeneous current distribution over the electrode surfaces. The limiting parameters of electrodeposition leads to the co-deposition of unwanted metals. Therefore, fine control of limitations is necessary to achieve high purity metals from the leachates derived from e-waste in an economically viable way. Further research on efficient sorting tools, selective and efficient leaching process and specific metal recovery processes that consider environmental and cost-benefit aspects, are required to address the current challenges of low recovery yield and high incurring cost and the operational feasibility of e-waste recycling technology.

**Author Contributions:** V.R., literature research, writing—first draft; D.L., literature search, writing—first draft; D.X., literature search, writing—first draft; Y.J., literature search, writing—review and editing; J.-C.P.G., Literature search, writing—review and editing, project administration and funding acquisition. All authors have read and agreed to the published version of the manuscript.

**Funding:** V.R., L.D.B., D.X., and Y.J. acknowledge the financial support from the NTU Singapore CEA Alliance for Research on the Circular Economy (SCARCE) project, which is supported by the National Research Foundation, Prime Minister’s Office, Singapore, the Ministry of National Development, Singapore, and the Ministry of Sustainability and the Environment, Singapore under the Closing the Waste Loop R&D Initiative as part of the Urban Solutions & Sustainability—Integration Fund (Award No. USS-IF-2018-4).

**Institutional Review Board Statement:** Not applicable.

**Informed Consent Statement:** Not applicable.

**Data Availability Statement:** Not applicable.

**Conflicts of Interest:** The authors declare no conflict of interest.

## References

1. Yang, J.; Wang, H.; Zhang, G.; Bai, X.; Zhao, X.; He, Y. Recycling organics from non-metallic fraction of waste printed circuit boards by a novel conical surface triboelectric separator. *Resour. Conserv. Recycl.* **2019**, *146*, 264–269. [[CrossRef](#)]
2. Forti, V.; Baldé, C.P.; Kuehr, R.; Bel, G. *The Global E-Waste Monitor 2020: Quantities, Flows and the Circular Economy Potential*; United Nations University (UNU)/United Nations Institute for Training and Research (UNITAR)—Co-hosted SCYCLE Programme, International Telecommunication Union (ITU) & International Solid Waste Association (ISWA): Bonn, Germany; Geneva, Switzerland; Rotterdam, The Netherlands, 2020.
3. Jin, W.; Hu, M.; Hu, J. Selective and Efficient Electrochemical Recovery of Dilute Copper and Tellurium from Acidic Chloride Solutions. *ACS Sustain. Chem. Eng.* **2018**, *6*, 13378–13384. [[CrossRef](#)]
4. Rai, V.; Tiwari, N.; Rajput, M.; Joshi, S.; Nguyen, A.C.; Mathews, N. Reversible Electrochemical Silver Deposition over Large Areas for Smart Windows and Information Display. *Electrochim. Acta* **2017**, *255*, 63–71. [[CrossRef](#)]
5. Rai, V.; Toh, C.-S. Electrochemical Amplification Strategies in DNA Nanosensors. *Nanosci. Nanotechnol. Lett.* **2013**, *5*, 613–623. [[CrossRef](#)]
6. Clevenger, T.E.; Novak, J.T. Recovery of Metals from Electroplating Wastes Using Liquid-Liquid Extraction. *J. Water Pollut. Control Fed.* **1983**, *55*, 984–989.

7. Deng, S.; Zhang, D.; Zhou, J.; Liu, H. Recycling of waste printed circuit board and preparation of high strength high purity copper foil by electrochemical method. *Xiyou Jinshu/Chin. J. Rare Met.* **2016**, *40*, 914–921. [[CrossRef](#)]
8. Ghosh, B.; Ghosh, M.; Parhi, P.; Mukherjee, P.; Mishra, B. Waste Printed Circuit Boards recycling: An extensive assessment of current status. *J. Clean. Prod.* **2015**, *94*, 5–19. [[CrossRef](#)]
9. Rao, M.D.; Singh, K.K.; Morrison, C.A.; Love, J.B. Challenges and opportunities in the recovery of gold from electronic waste. *RSC Adv.* **2020**, *10*, 4300–4309. [[CrossRef](#)]
10. Sethurajan, M.; van Hullebusch, E.D.; Fontana, D.; Akcil, A.; Deveci, H.; Batinic, B.; Leal, J.; Gasche, T.A.; Kucuker, M.A.; Kuchta, K.; et al. Recent advances on hydrometallurgical recovery of critical and precious elements from end of life electronic wastes—A review. *Crit. Rev. Environ. Sci. Technol.* **2019**, *49*, 212–275. [[CrossRef](#)]
11. Faraji, F.; Alizadeh, A.; Rashchi, F.; Mostoufi, N. Kinetics of leaching: A review. *Rev. Chem. Eng.* **2019**. [[CrossRef](#)]
12. Sun, C.-B.; Zhang, X.-L.; Kou, J.; Xing, Y. A review of gold extraction using noncyanide lixiviants: Fundamentals, advancements, and challenges toward alkaline sulfur-containing leaching agents. *Int. J. Miner. Met. Mater.* **2020**, *27*, 417–431. [[CrossRef](#)]
13. Hubau, A.; Chagnes, A.; Minier, M.; Touzé, S.; Chapron, S.; Guezenec, A.-G. Recycling-oriented methodology to sample and characterize the metal composition of waste Printed Circuit Boards. *Waste Manag.* **2019**, *91*, 62–71. [[CrossRef](#)] [[PubMed](#)]
14. Aliakbari, R.; Marfavi, Y.; Kowsari, E.; Ramakrishna, S. Recent Studies on Ionic Liquids in Metal Recovery from E-Waste and Secondary Sources by Liquid-Liquid Extraction and Electrodeposition: A Review. *Mater. Circ. Econ.* **2020**, *2*, 1–27. [[CrossRef](#)]
15. Gamburg, Y.D. New Ideas And Results in Electrochemical Crystallization and Deposition of Metals. In *Metal Electrodeposition*; Nunez, M., Ed.; Nova Science Publishers, Inc.: New York, NY, USA, 2005; pp. 47–77.
16. Jari Aromaa, D.S. Aqueous Processing of Metals. In *Encyclopedia of Electrochemistry*; Wiley: Weinheim, Germany, 2007; pp. 161–223.
17. Diaz, L.A.; Lister, T.E. Economic evaluation of an electrochemical process for the recovery of metals from electronic waste. *Waste Manag.* **2018**, *74*, 384–392. [[CrossRef](#)]
18. Diaz, L.A.; Lister, T.E.; Parkman, J.A.; Clark, G.G. Comprehensive process for the recovery of value and critical materials from electronic waste. *J. Clean. Prod.* **2016**, *125*, 236–244. [[CrossRef](#)]
19. Li, Z.; Diaz, L.A.; Yang, Z.; Jin, H.; Lister, T.E.; Vahidi, E.; Zhao, F. Comparative life cycle analysis for value recovery of precious metals and rare earth elements from electronic waste. *Resour. Conserv. Recycl.* **2019**, *149*, 20–30. [[CrossRef](#)]
20. Chapter 6 Copper Production Technology. Available online: <https://www.princeton.edu/~ota/disk2/1988/8808/880808> (accessed on 5 August 2021).
21. Kaya, M. Recovery of metals and nonmetals from electronic waste by physical and chemical recycling processes. *Waste Manag.* **2016**, *57*, 64–90. [[CrossRef](#)]
22. Cui, J.; Forssberg, E. Mechanical recycling of waste electric and electronic equipment: A review. *J. Hazard. Mater.* **2003**, *99*, 243–263. [[CrossRef](#)]
23. Yazici, E.; Deveci, H. Extraction of metals from waste printed circuit boards (WPCBs) in H<sub>2</sub>SO<sub>4</sub>–CuSO<sub>4</sub>–NaCl solutions. *Hydrometallurgy* **2013**, *139*, 30–38. [[CrossRef](#)]
24. Ogunniyi, I.; Vermaak, M.; Groot, D. Chemical composition and liberation characterization of printed circuit board comminution fines for beneficiation investigations. *Waste Manag.* **2009**, *29*, 2140–2146. [[CrossRef](#)] [[PubMed](#)]
25. Bizzo, W.A.; Figueiredo, R.A.; De Andrade, V.F. Characterization of Printed Circuit Boards for Metal and Energy Recovery after Milling and Mechanical Separation. *Materials* **2014**, *7*, 4555–4566. [[CrossRef](#)] [[PubMed](#)]
26. Bernasconi, R.; Panzeri, G.; Accogli, A.; Liberale, F.; Nobili, L.; Magagnin, L. Electrodeposition from Deep Eutectic Solvents. In *Progress and Developments in Ionic Liquids*; InTech: London, UK, 2017; p. 236.
27. Maniam, K.K.; Paul, S. A Review on the Electrodeposition of Aluminum and Aluminum Alloys in Ionic Liquids. *Coatings* **2021**, *11*, 80. [[CrossRef](#)]
28. Abbott, A.P.; McKenzie, K.J. Application of ionic liquids to the electrodeposition of metals. *Phys. Chem. Chem. Phys.* **2006**, *8*, 4265–4279. [[CrossRef](#)] [[PubMed](#)]
29. Zhang, Q.; Hua, Y.; Xu, C.; Li, Y.; Li, J.; Dong, P. Non-haloaluminate ionic liquids for low-temperature electrodeposition of rare-earth metals—A review. *J. Rare Earths* **2015**, *33*, 1017–1025. [[CrossRef](#)]
30. Lu, Y.; Xu, Z. Precious metals recovery from waste printed circuit boards: A review for current status and perspective. *Resour. Conserv. Recycl.* **2016**, *113*, 28–39. [[CrossRef](#)]
31. Feldman, A.V. Method for Processing Scrap of Electronic Instruments. U.S. Patent 5,217,171, 8 June 1993.
32. Menetti, R.P.; Tenório, S.A.J. Recycling of Precious Metals from Electronic Scraps. In Proceedings of the 50th Annual Congress of ABM, São Pedro, SP, Brazil, 1–4 August 1995; pp. 625–634. (In Portuguese).
33. Iji, M.; Yokoyama, S. Recycling of Printed Wiring Boards with Mounted Electronic Components. *Circ. World* **1997**, *23*, 10–15. [[CrossRef](#)]
34. Veit, H.M.; De Pereira, C.C.; Bernardes, A.M. Using mechanical processing in recycling printed wiring boards. *JOM* **2002**, *54*, 45–47. [[CrossRef](#)]
35. Zhao, Y.; Wen, X.; Li, B.; Tao, D. Recovery of copper from waste printed circuit boards. *Min. Met. Explor.* **2004**, *21*, 99–102. [[CrossRef](#)]
36. Kim, B.-S.; Lee, J.-C.; Seo, S.-P.; Park, Y.-K.; Sohn, H.Y. A process for extracting precious metals from spent printed circuit boards and automobile catalysts. *JOM* **2004**, *56*, 55–58. [[CrossRef](#)]

37. Wang, H.; Gu, G.-H.; Qi, Y.-F. Crushing performance and resource characteristic of printed circuit board scrap. *J. Cent. South Univ. Technol.* **2005**, *12*, 552–555. [[CrossRef](#)]
38. Creamer, N.J.; Baxter-Plant, V.S.; Henderson, J.; Potter, M.; Macaskie, L.E. Palladium and gold removal and recovery from precious metal solutions and electronic scrap leachates by *Desulfovibrio desulfuricans*. *Biotechnol. Lett.* **2006**, *28*, 1475–1484. [[CrossRef](#)] [[PubMed](#)]
39. De Marco, I.; Caballero, B.; Chomón, M.; Laresgoiti, M.; Torres, A.; Fernández, G.; Arnaiz, S. Pyrolysis of electrical and electronic wastes. *J. Anal. Appl. Pyrolysis* **2008**, *82*, 179–183. [[CrossRef](#)]
40. Hino, T.; Agawa, R.; Moriya, Y.; Nishida, M.; Tsugita, Y.; Araki, T. Techniques to separate metal from waste printed circuit boards from discarded personal computers. *J. Mater. Cycles Waste Manag.* **2009**, *11*, 42–54. [[CrossRef](#)]
41. Das, A.; Vidyadhar, A.; Mehrotra, S. A novel flowsheet for the recovery of metal values from waste printed circuit boards. *Resour. Conserv. Recycl.* **2009**, *53*, 464–469. [[CrossRef](#)]
42. Yoo, J.-M.; Jeong, J.; Yoo, K.; Lee, J.-C.; Kim, W. Enrichment of the metallic components from waste printed circuit boards by a mechanical separation process using a stamp mill. *Waste Manag.* **2009**, *29*, 1132–1137. [[CrossRef](#)]
43. Oliveira, P.C.; Cabral, M.; Nogueira, C.; Margarido, F. Printed Circuit Boards Recycling: Characterization of Granulometric Fractions from Shredding Process. *Mater. Sci. Forum* **2010**, *636–637*, 1434–1439. [[CrossRef](#)]
44. Oulmas, C.; Mameri, S.; Boughrara, D.; Kadri, A.; Delhalle, J.; Mekhalif, Z.; Benfedda, B. Comparative study of Cu–Zn coatings electrodeposited from sulphate and chloride baths. *Heliyon* **2019**, *5*, e02058. [[CrossRef](#)] [[PubMed](#)]
45. Jiang, T.; Brym, M.C.; Dubé, G.; Lasia, A.; Brisard, G. Electrodeposition of aluminium from ionic liquids: Part I—electrodeposition and surface morphology of aluminium from aluminium chloride (AlCl<sub>3</sub>)–1-ethyl-3-methylimidazolium chloride ([EMIm]Cl) ionic liquids. *Surf. Coatings Technol.* **2006**, *201*, 1–9. [[CrossRef](#)]
46. Birlik, I.; Azem, N.F.A. Influence of Bath Composition on the Structure and Properties of Nickel Coatings Produced by Electrodeposition Technique. *Deu Muhendis. Fak. Fen Muhendis.* **2018**, *20*, 689–697. [[CrossRef](#)]
47. Zhang, Z.; Kitada, A.; Fukami, K.; Yao, Z.; Murase, K. Electrodeposition of an iron thin film with compact and smooth morphology using an ethereal electrolyte. *Electrochim. Acta* **2020**, *348*, 136289. [[CrossRef](#)]
48. He, A.; Liu, Q.; Ivey, D.G. Electrodeposition of tin: A simple approach. *J. Mater. Sci. Mater. Electron.* **2007**, *19*, 553–562. [[CrossRef](#)]
49. Zhao, L.Y.; Siu, A.C.; Pariag, L.J.; He, Z.H.; Leung, K.T. Electrochemical Deposition of Chromium Core–Shell Nanostructures on H–Si(100): Evolution of Spherical Nanoparticles to Uniform Thin Film without and with Atop Hexagonal Microrods. *J. Phys. Chem. C* **2007**, *111*, 14621–14624. [[CrossRef](#)]
50. Akben, H.K.; Timur, S.I. A comparative study of silver electrodeposition from pyrophosphate-cyanide and high concentration cyanide electrolytes in the presence of brighteners. *Turk. J. Chem.* **2020**, *44*, 378–392. [[CrossRef](#)] [[PubMed](#)]
51. Lahiri, A.; Pulletikurthi, G.; Endres, F. A Review on the Electroless Deposition of Functional Materials in Ionic Liquids for Batteries and Catalysis. *Front. Chem.* **2019**, *7*, 7. [[CrossRef](#)] [[PubMed](#)]
52. Yu, P.; Yan, J.; Zhang, J.; Mao, L. Cost-effective electrodeposition of platinum nanoparticles with ionic liquid droplet confined onto electrode surface as micro-media. *Electrochem. Commun.* **2007**, *9*, 1139–1144. [[CrossRef](#)]
53. Asnavandi, M.; Suryanto, B.; Zhao, C. Controlled electrodeposition of nanostructured Pd thin films from protic ionic liquids for electrocatalytic oxygen reduction reactions. *RSC Adv.* **2015**, *5*, 74017–74023. [[CrossRef](#)]
54. Mukhopadhyay, I.; Aravinda, C.; Borissov, D.; Freyland, W. Electrodeposition of Ti from TiCl<sub>4</sub> in the ionic liquid 1-methyl-3-butyl-imidazolium bis (trifluoro methyl sulfone) imide at room temperature: Study on phase formation by in situ electrochemical scanning tunneling microscopy. *Electrochim. Acta* **2005**, *50*, 1275–1281. [[CrossRef](#)]
55. Maarof, H.I.; Daud, W.M.A.W.; Aroua, M.K. Recent trends in removal and recovery of heavy metals from wastewater by electrochemical technologies. *Rev. Chem. Eng.* **2016**, *33*, 359–386. [[CrossRef](#)]
56. Jayakrishnan, D.S. Electrodeposition: The Versatile Technique for Nanomaterials. In *Corrosion Protection and Control Using Nanomaterials*; Saji, V.S., Cook, R., Eds.; Woodhead Publishing: Cambridge, UK, 2012; pp. 86–125.
57. De la Prida, V.; Vega, V.; Garcia, J.M.V.; Iglesias, L.L.; Hernando, B.; Minguez-Bacho, I. Electrochemical methods for template-assisted synthesis of nanostructured materials. In *Magnetic Nano-and Microwires*; Vázquez, M., Ed.; Woodhead Publishing: Amsterdam, The Netherlands, 2015; pp. 3–39.
58. Hussein, H.E.M.; Maurer, R.J.; Amari, H.; Peters, J.; Meng, L.; Beanland, R.; Newton, M.E.; MacPherson, J.V. Tracking Metal Electrodeposition Dynamics from Nucleation and Growth of a Single Atom to a Crystalline Nanoparticle. *ACS Nano* **2018**, *12*, 7388–7396. [[CrossRef](#)] [[PubMed](#)]
59. Nasirpouri, F. Fundamentals and Principles of Electrode-Position. In *Electrodeposition of Nanostructured Materials*; Springer International Publishing: Cham, Germany, 2017; pp. 75–121.
60. Batail, P.; Boubekeur, K.; Fourmigué, M.; Gabriel, J.-C.P. Electrocrystallization, an Invaluable Tool for the Construction of Ordered, Electroactive Molecular Solids<sup>†</sup>. *Chem. Mater.* **1998**, *10*, 3005–3015. [[CrossRef](#)]
61. Kowalska, S.; Lukomska, A.; Łoś, P.; Chmielewski, T.; Wozniak, B. Potential-controlled electrolysis as an effective method of selective silver electrowinning from complex matrix leaching solutions of copper concentrate. *Int. J. Electrochem. Sci.* **2015**, *10*, 1186–1198.
62. Liu, Y.; Zhang, L.; Song, Q.; Xu, Z. Recovery of palladium as nanoparticles from waste multilayer ceramic capacitors by potential-controlled electrodeposition. *J. Clean. Prod.* **2020**, *257*, 120370. [[CrossRef](#)]

63. Sun, Z.; Xiao, Y.; Sietsma, J.; Agterhuis, H.; Yang, Y. A Cleaner Process for Selective Recovery of Valuable Metals from Electronic Waste of Complex Mixtures of End-of-Life Electronic Products. *Environ. Sci. Technol.* **2015**, *49*, 7981–7988. [[CrossRef](#)] [[PubMed](#)]
64. Haccuria, E.; Ning, P.; Cao, H.; Venkatesan, P.; Jin, W.; Yang, Y.; Sun, Z. Effective treatment for electronic waste—Selective recovery of copper by combining electrochemical dissolution and deposition. *J. Clean. Prod.* **2017**, *152*, 150–156. [[CrossRef](#)]
65. Xu, X.; Sturm, S.; Samardzija, Z.; Scancar, J.; Markovic, K.; Rozman, K.Z. A facile method for the simultaneous recovery of rare-earth elements and transition metals from Nd–Fe–B magnets. *Green Chem.* **2020**, *22*, 1105–1112. [[CrossRef](#)]
66. Koene, L.; Janssen, L. Removal of nickel from industrial process liquids. *Electrochim. Acta* **2001**, *47*, 695–703. [[CrossRef](#)]
67. Abou-Shady, A.; Peng, C.; Bi, J.; Xu, H.; Almeria, O.J. Recovery of Pb (II) and removal of NO<sub>3</sub><sup>−</sup> from aqueous solutions using integrated electrodialysis, electrolysis, and adsorption process. *Desalination* **2012**, *286*, 304–315. [[CrossRef](#)]
68. Peng, C.; Jin, R.; Li, G.; Li, F.; Gu, Q. Recovery of nickel and water from wastewater with electrochemical combination process. *Sep. Purif. Technol.* **2014**, *136*, 42–49. [[CrossRef](#)]
69. Zhang, X.; Yang, F.; Ma, J.; Liang, P. Effective removal and selective capture of copper from salty solution in flow electrode capacitive deionization. *Environ. Sci. Water Res. Technol.* **2019**, *6*, 341–350. [[CrossRef](#)]
70. Chandrasekar, M.; Pushpavanam, M. Pulse and pulse reverse plating—Conceptual, advantages and applications. *Electrochim. Acta* **2008**, *53*, 3313–3322. [[CrossRef](#)]
71. Balasubramanian, A.; Srikumar, D.S.; Raja, G.; Saravanan, G.; Mohan, S. Effect of pulse parameter on pulsed electrodeposition of copper on stainless steel. *Surf. Eng.* **2009**, *25*, 389–392. [[CrossRef](#)]
72. Gao, Y.; Zhou, Y.; Wang, H.; Lin, W.; Wang, Y.; Sun, D.; Hong, J.; Li, Q. Simultaneous Silver Recovery and Cyanide Removal from Electroplating Wastewater by Pulse Current Electrolysis Using Static Cylinder Electrodes. *Ind. Eng. Chem. Res.* **2013**, *52*, 5871–5879. [[CrossRef](#)]
73. Qiang, L.; Pinto, I.; Youcai, Z. Sequential stepwise recovery of selected metals from flue dusts of secondary copper smelting. *J. Clean. Prod.* **2014**, *84*, 663–670. [[CrossRef](#)]
74. Su, Y.-B.; Li, Q.-B.; Wang, Y.-P.; Wang, H.-T.; Huang, J.; Yang, X. Electrochemical reclamation of silver from silver-plating wastewater using static cylinder electrodes and a pulsed electric field. *J. Hazard. Mater.* **2009**, *170*, 1164–1172. [[CrossRef](#)]
75. Hannula, P.-M.; Khalid, M.K.; Janas, D.; Yliniemi, K.; Lundström, M. Energy efficient copper electrowinning and direct deposition on carbon nanotube film from industrial wastewaters. *J. Clean. Prod.* **2019**, *207*, 1033–1039. [[CrossRef](#)]
76. Subbaiah, T.; Singh, P.; Hefter, G.; Muir, D.; Das, R.P. Electrowinning of Copper in the Presence of Anodic Depolarisers—A Review. *Miner. Process. Extr. Met. Rev.* **2000**, *21*, 479–496. [[CrossRef](#)]
77. Koo, J.-K.; Hong, H.-K.; Lee, J.-H. Recovery of Bi and Sb from Copper Spent Electrolytes by Electrowinning Method. *J. Nanosci. Nanotechnol.* **2015**, *15*, 8943–8946. [[CrossRef](#)]
78. Thanu, V.C.; Jayakumar, M. Electrochemical recovery of antimony and bismuth from spent electrolytes. *Sep. Purif. Technol.* **2020**, *235*, 116169. [[CrossRef](#)]
79. Cao, X.; Dreisinger, D.B.; Lu, J.; Belanger, F. Electrorefining of high purity manganese. *Hydrometallurgy* **2017**, *171*, 412–421. [[CrossRef](#)]
80. Cui, J.; Zhang, L. Metallurgical recovery of metals from electronic waste: A review. *J. Hazard. Mater.* **2008**, *158*, 228–256. [[CrossRef](#)] [[PubMed](#)]
81. Li, F.; Chen, M.; Shu, J.; Shirvani, M.; Li, Y.; Sun, Z.; Sun, S.; Xu, Z.; Fu, K.; Chen, S. Copper and gold recovery from CPU sockets by one-step slurry electrolysis. *J. Clean. Prod.* **2019**, *213*, 673–679. [[CrossRef](#)]
82. Oishi, T.; Koyama, K.; Konishi, H.; Tanaka, M.; Lee, J.-C. Influence of ammonium salt on electrowinning of copper from ammoniacal alkaline solutions. *Electrochim. Acta* **2007**, *53*, 127–132. [[CrossRef](#)]
83. Dong, B.; Fishgold, A.; Lee, P.; Runge, K.; Deymier, P.; Keswani, M. Sono-electrochemical recovery of metal ions from their aqueous solutions. *J. Hazard. Mater.* **2016**, *318*, 379–387. [[CrossRef](#)]
84. Radziuk, D.; Möhwald, H. Ultrasonically treated liquid interfaces for progress in cleaning and separation processes. *Phys. Chem. Chem. Phys.* **2015**, *18*, 21–46. [[CrossRef](#)]
85. Li, H.; Eksteen, J.; Oraby, E. Hydrometallurgical recovery of metals from waste printed circuit boards (WPCBs): Current status and perspectives—A review. *Resour. Conserv. Recycl.* **2018**, *139*, 122–139. [[CrossRef](#)]
86. Oishi, T.; Koyama, K.; Alam, S.; Tanaka, M.; Lee, J.-C. Recovery of high purity copper cathode from printed circuit boards using ammoniacal sulfate or chloride solutions. *Hydrometallurgy* **2007**, *89*, 82–88. [[CrossRef](#)]
87. Joda, N.N.; Rashchi, F. Recovery of ultra fine grained silver and copper from PC board scraps. *Sep. Purif. Technol.* **2012**, *92*, 36–42. [[CrossRef](#)]
88. Mecucci, A.; Scott, K. Leaching and electrochemical recovery of copper, lead and tin from scrap printed circuit boards. *J. Chem. Technol. Biotechnol.* **2002**, *77*, 449–457. [[CrossRef](#)]
89. Leclerc, N.; Legeai, S.; Balva, M.; Hazotte, C.; Comel, J.; Lopicque, F.; Billy, E.; Meux, E. Recovery of Metals from Secondary Raw Materials by Coupled Electroleaching and Electrodeposition in Aqueous or Ionic Liquid Media. *Metals* **2018**, *8*, 556. [[CrossRef](#)]
90. Fogarasi, S.; Imre-Lucaci, F.; Fogarasi, M.; Imre-Lucaci, Á. Technical and environmental assessment of selective recovery of tin and lead from waste solder alloy using direct anodic oxidation. *J. Clean. Prod.* **2019**, *213*, 872–883. [[CrossRef](#)]
91. Veit, H.M.; Bernardes, A.M.; Ferreira, J.Z.; Ten'orio, J.Z.F.; Malfatti, C. Recovery of copper from printed circuit boards scraps by mechanical processing and electrometallurgy. *J. Hazard. Mater.* **2006**, *137*, 1704–1709. [[CrossRef](#)] [[PubMed](#)]

92. Fogarasi, S.; Imre-Lucaci, F.; Egedy, A.; Imre-Lucaci, Á.; Ilea, P. Eco-friendly copper recovery process from waste printed circuit boards using  $\text{Fe}^{3+}/\text{Fe}^{2+}$  redox system. *Waste Manag.* **2015**, *40*, 136–143. [[CrossRef](#)] [[PubMed](#)]
93. Matsumiya, M.; Sumi, M.; Uchino, Y.; Yanagi, I. Recovery of indium based on the combined methods of ionic liquid extraction and electrodeposition. *Sep. Purif. Technol.* **2018**, *201*, 25–29. [[CrossRef](#)]
94. Zhang, Q.; Wang, Q.; Zhang, S.; Lu, X.; Zhang, X. Electrodeposition in Ionic Liquids. *ChemPhysChem* **2015**, *17*, 335–351. [[CrossRef](#)] [[PubMed](#)]
95. Abbott, A.P.; Capper, G.; McKenzie, K.J.; Ryder, K. Electrodeposition of zinc–tin alloys from deep eutectic solvents based on choline chloride. *J. Electroanal. Chem.* **2007**, *599*, 288–294. [[CrossRef](#)]
96. Gomez, E.; Cojocar, P.; Magagnin, L.; Vallés, E. Electrodeposition of Co, Sm and SmCo from a Deep Eutectic Solvent. *J. Electroanal. Chem.* **2011**, *658*, 18–24. [[CrossRef](#)]
97. Abbott, A.; Ballantyne, A.; Harris, R.; Juma, J.A.; Ryder, K.; Forrest, G. A Comparative Study of Nickel Electrodeposition Using Deep Eutectic Solvents and Aqueous Solutions. *Electrochim. Acta* **2015**, *176*, 718–726. [[CrossRef](#)]
98. Simka, W.; Puszczuk, D.; Nawrat, G. Electrodeposition of metals from non-aqueous solutions. *Electrochim. Acta* **2009**, *54*, 5307–5319. [[CrossRef](#)]
99. He, J.; Yang, J.; Tariq, S.M.; Duan, C.; Zhao, Y. Comparative investigation on copper leaching efficiency from waste mobile phones using various types of ionic liquids. *J. Clean. Prod.* **2020**, *256*, 120368. [[CrossRef](#)]
100. Zante, G.; Braun, A.; Masmoudi, A.; Barillon, R.; Trébouet, D.; Boltoeva, M. Solvent extraction fractionation of manganese, cobalt, nickel and lithium using ionic liquids and deep eutectic solvents. *Miner. Eng.* **2020**, *156*, 106512. [[CrossRef](#)]
101. El Abedin, S.Z.; Endres, F. Electrodeposition of Metals and Semiconductors in Air- and Water-Stable Ionic Liquids. *ChemPhysChem* **2006**, *7*, 58–61. [[CrossRef](#)] [[PubMed](#)]
102. Kamimoto, Y.; Itoh, T.; Yoshimura, G.; Kuroda, K.; Hagio, T.; Ichino, R. Electrodeposition of rare-earth elements from neodymium magnets using molten salt electrolysis. *J. Mater. Cycles Waste Manag.* **2018**, *20*, 1918–1922. [[CrossRef](#)]
103. Abbasalizadeh, A.; Malfliet, A.; Seetharaman, S.; Sietsma, J.; Yang, Y. Electrochemical Recovery of Rare Earth Elements from Magnets: Conversion of Rare Earth Based Metals into Rare Earth Fluorides in Molten Salts. *Mater. Trans.* **2017**, *58*, 400–405. [[CrossRef](#)]
104. Martinez, A.M.; Kjos, O.; Skybakmoen, E.; Solheim, A.; Haarberg, G.M. Extraction of rare earth metals from Nd-based scrap by electrolysis from molten salts. *ECS Trans.* **2012**, *50*, 453–461. [[CrossRef](#)]
105. Yang, Y.; Lan, C.; Guo, L.; An, Z.; Zhao, Z.; Li, B. Recovery of rare-earth element from rare-earth permanent magnet waste by electro-refining in molten fluorides. *Sep. Purif. Technol.* **2020**, *233*, 116030. [[CrossRef](#)]
106. Grinberg, V.; Mazin, V. Electrochemical processes in liquid and supercritical carbon dioxide. *Russ. J. Electrochem.* **1998**, *34*, 223–229.
107. Abbott, A.; Eardley, C.A. Solvent Properties of Liquid and Supercritical Hydrofluorocarbons. *J. Phys. Chem. B* **1999**, *103*, 2504–2509. [[CrossRef](#)]
108. Blackburn, J.M.; Long, D.P.; Cabañas, A.; Watkins, J.J. Deposition of Conformal Copper and Nickel Films from Supercritical Carbon Dioxide. *Science* **2001**, *294*, 141–145. [[CrossRef](#)]
109. Toghiani, K.; Méndez, M.A.; Voyame, P. Electrochemistry in supercritical fluids: A mini review. *Electrochem. Commun.* **2014**, *44*, 27–30. [[CrossRef](#)]
110. Branch, J.A.; Bartlett, P.N. Electrochemistry in supercritical fluids. *Philos. Trans. R. Soc. A Math. Phys. Eng. Sci.* **2015**, *373*, 20150007. [[CrossRef](#)]
111. Bartlett, P.N.; Cook, D.A.; George, M.W.; Hector, A.L.; Ke, J.; Levason, W.; Reid, G.; Smith, D.C.; Zhang, W. Electrodeposition from supercritical fluids. *Phys. Chem. Chem. Phys.* **2014**, *16*, 9202–9219. [[CrossRef](#)]
112. Ke, J.; Bartlett, P.N.; Cook, D.; Easun, T.L.; George, M.W.; Levason, W.; Reid, G.; Smith, D.; Su, W.; Zhang, W. Electrodeposition of germanium from supercritical fluids. *Phys. Chem. Chem. Phys.* **2011**, *14*, 1517–1528. [[CrossRef](#)]
113. McDonald, A.C.; Fan, F.R.F.; Bard, A.J. Electrochemistry in near-critical and supercritical fluids. Water. Experimental techniques and the copper(II) system. *J. Phys. Chem.* **1986**, *90*, 196–202. [[CrossRef](#)]
114. Abbott, A.P.; Harper, J.C. Electrochemical investigations in supercritical carbon dioxide. *J. Chem. Soc. Faraday Trans.* **1996**, *92*, 3895–3898. [[CrossRef](#)]
115. Ursov, E.D.; Kondratenko, M.S.; Gallyamov, M.O. Platinum Electrodeposition from a Carbon Dioxide-Based Supercritical Electrolyte. *Dokl. Phys. Chem.* **2019**, *489*, 173–176. [[CrossRef](#)]
116. Ke, J.; Su, W.; Howdle, S.; George, M.W.; Cook, D.; Perdjon-Abel, M.; Bartlett, P.N.; Zhang, W.; Cheng, F.; Levason, W.; et al. Electrodeposition of metals from supercritical fluids. *Proc. Natl. Acad. Sci. USA* **2009**, *106*, 14768–14772. [[CrossRef](#)]
117. Cook, D.; Bartlett, P.N.; Zhang, W.; Levason, W.; Reid, G.; Ke, J.; Su, W.; George, M.W.; Wilson, J.; Smith, D.; et al. The electrodeposition of copper from supercritical  $\text{CO}_2$ /acetonitrile mixtures and from supercritical trifluoromethane. *Phys. Chem. Chem. Phys.* **2010**, *12*, 11744–11752. [[CrossRef](#)] [[PubMed](#)]
118. Champion, M.J.D.; Levason, W.; Pugh, D.; Reid, G. Hexahalometallate salts of trivalent scandium, yttrium and lanthanum: Cation–anion association in the solid state and in solution. *New J. Chem.* **2016**, *40*, 7181–7189. [[CrossRef](#)]
119. Han, X.; Ke, J.; Suleiman, N.; Levason, W.; Pugh, D.; Zhang, W.; Reid, G.; Licence, P.; George, M.W. Phase behaviour and conductivity of supporting electrolytes in supercritical difluoromethane and 1,1-difluoroethane. *Phys. Chem. Chem. Phys.* **2016**, *18*, 14359–14369. [[CrossRef](#)] [[PubMed](#)]

120. Bartlett, P.N.; Burt, J.; Cook, D.A.; Cummings, C.Y.; George, M.W.; Hector, A.L.; Hasan, M.M.; Ke, J.; Levason, W.; Pugh, D.; et al. A Versatile Precursor System for Supercritical Fluid Electrodeposition of Main-Group Materials. *Chem. A Eur. J.* **2015**, *22*, 302–309. [[CrossRef](#)] [[PubMed](#)]
121. Cummings, C.Y.; Bartlett, P.N.; Pugh, D.; Reid, G.; Levason, W.; Hasan, M.M.; Hector, A.L.; Spencer, J.; Smith, D.C.; Marks, S.; et al. Electrodeposition of Protocrystalline Germanium from Supercritical Difluoromethane. *ChemElectroChem* **2016**, *3*, 726–733. [[CrossRef](#)]
122. Bartlett, P.N.; Cook, D.A.; Hasan, M.M.; Hector, A.L.; Marks, S.; Naik, J.; Reid, G.; Sloan, J.; Smith, D.C.; Spencer, J.; et al. Supercritical fluid electrodeposition, structural and electrical characterisation of tellurium nanowires. *RSC Adv.* **2017**, *7*, 40720–40726. [[CrossRef](#)]
123. Lodge, A.W.; Hasan, M.M.; Bartlett, P.N.; Beanland, R.; Hector, A.L.; Kashtiban, R.J.; Levason, W.; Reid, G.; Sloan, J.; Smith, D.C.; et al. Electrodeposition of tin nanowires from a dichloromethane based electrolyte. *RSC Adv.* **2018**, *8*, 24013–24020. [[CrossRef](#)]
124. Bartlett, P.N.; Beanland, R.; Burt, J.; Hasan, M.M.; Hector, A.L.; Kashtiban, R.J.; Levason, W.; Lodge, A.W.; Marks, S.; Naik, J.; et al. Exploration of the Smallest Diameter Tin Nanowires Achievable with Electrodeposition: Sub 7 nm Sn Nanowires Produced by Electrodeposition from a Supercritical Fluid. *Nano Lett.* **2018**, *18*, 941–947. [[CrossRef](#)] [[PubMed](#)]
125. Wang, J. Electrochemical biosensors: Towards point-of-care cancer diagnostics. *Biosens. Bioelectron.* **2006**, *21*, 1887–1892. [[CrossRef](#)] [[PubMed](#)]
126. Lu, W.; Lieber, C.M.; Rodgers, P. Nanoelectronics from the bottom up. *Nanosci. Technol.* **2009**, 137–146. [[CrossRef](#)]
127. Zhang, Y.; Erkey, C. Preparation of supported metallic nanoparticles using supercritical fluids: A review. *J. Supercrit. Fluids* **2006**, *38*, 252–267. [[CrossRef](#)]
128. Erkey, C. Preparation of metallic supported nanoparticles and films using supercritical fluid deposition. *J. Supercrit. Fluids* **2009**, *47*, 517–522. [[CrossRef](#)]
129. Tang, H.-C.; Chen, C.-Y.; Nagoshi, T.; Chang, T.-F.M.; Yamane, D.; Machida, K.; Masu, K.; Sone, M. Enhancement of mechanical strength in Au films electroplated with supercritical carbon dioxide. *Electrochem. Commun.* **2016**, *72*, 126–130. [[CrossRef](#)]
130. Liu, C.; Su, F.; Liang, J. Corrosion and Wear Behavior of Sc-CO<sub>2</sub> Assisted-Deposition Nanocrystalline Co Film in Simulated Body Fluid. *J. Electrochem. Soc.* **2016**, *163*, D585–D591. [[CrossRef](#)]
131. Liu, W.Q.; Lei, W.N.; Shen, Y.; Wang, C.Y.; Qian, H.F.; Li, Q.L. Performance characterization and preparation of Ni-SiC nanocomposites based on SCF-CO<sub>2</sub>. *Integr. Ferroelectr.* **2017**, *179*, 45–55. [[CrossRef](#)]
132. Chuang, H.-C.; Sánchez, J.; Cheng, H.-Y. The Effect of Surfactant Content over Cu-Ni Coatings Electroplated by the sc-CO<sub>2</sub> Technique. *Materials* **2017**, *10*, 428. [[CrossRef](#)] [[PubMed](#)]
133. Chuang, H.-C.; Yang, H.-M.; Wu, G.-L.; Sanchez, J.; Shyu, J.-H. The effects of ultrasonic agitation on supercritical CO<sub>2</sub> copper electroplating. *Ultrason. Sonochem.* **2018**, *40*, 147–156. [[CrossRef](#)] [[PubMed](#)]
134. Chuang, H.-C.; Sanchez, J. Fabrication of Cu coatings by ultrasound-assisted supercritical argon electroplating. *Mater. Lett.* **2019**, *243*, 54–57. [[CrossRef](#)]
135. Chuang, H.-C.; Jiang, G.-W.; Sanchez, J. Study on the changes of ultrasonic parameters over supercritical Ni-Co electroplating process. *Ultrason. Sonochem.* **2020**, *60*, 104805. [[CrossRef](#)] [[PubMed](#)]
136. Liu, C.-S.; Su, F.-H.; Liang, J.-Z. Fabrication of Co–Ni–P film with excellent wear and corrosion resistance by electroplating with supercritical CO<sub>2</sub> emulsion. *Trans. Nonferrous Met. Soc. China* **2018**, *28*, 2489–2498. [[CrossRef](#)]
137. Chuang, H.-C.; Su, H.-C.; Sanchez, J. The characteristics of nickel film produced by supercritical carbon dioxide electroplating with ultrasonic agitation. *Ultrason. Sonochem.* **2019**, *57*, 48–56. [[CrossRef](#)] [[PubMed](#)]
138. Chuang, H.-C.; Sanchez, J. Parametric Characterization of Copper Metal Coatings Produced by Supercritical Argon Electroplating. *JOM* **2019**, *72*, 711–720. [[CrossRef](#)]
139. Lister, T.E.; Diaz, L.A.; Clark, G.G.; Keller, P. *Process Development for the Recovery of Critical Materials from Electronic Waste*; Idaho National Lab. (INL): Idaho Falls, ID, USA, 2016.
140. Kim, E.-Y.; Kim, M.-S.; Lee, J.-C.; Yoo, K.; Jeong, J. Leaching behavior of copper using electro-generated chlorine in hydrochloric acid solution. *Hydrometallurgy* **2010**, *100*, 95–102. [[CrossRef](#)]
141. Khaliq, A.; Rhamdhani, M.A.; Brooks, G.; Masood, S. Metal Extraction Processes for Electronic Waste and Existing Industrial Routes: A Review and Australian Perspective. *Resources* **2014**, *3*, 152–179. [[CrossRef](#)]